Does convection-permitting simulate better rainfall distribution and extreme over Guinean coast and surroundings?

Kouakou Kouadio, Sophie Bastin, Abdourahamane Konare, Vincent Ajayi

Climate Dynamics

Does convection-permitting simulate better rainfall distribution and extreme over Guinean coast and surroundings?
--Manuscript Draft--

Manuscript Number:	CLDY-D-17-00719R2
Full Title:	Does convection-permitting simulate better rainfall distribution and extreme over Guinean coast and surroundings?
Article Type:	S.I. : Advances in Convection-Permitting Climate Modeling
Keywords:	high resolution, WRF, West Africa monsoon, Parameterization, Rainfall, convection permitting
Corresponding Author:	kouakou kouadio, Ph.D Universite Felix Houphouet-Boigny Abidjan, abidjan CÔTE D'IVOIRE
Corresponding Author Secondary Information:	
Corresponding Author's Institution:	Universite Felix Houphouet-Boigny
Corresponding Author's Secondary Institution:	
First Author:	kouakou kouadio, Ph.D
First Author Secondary Information:	
Order of Authors:	kouakou kouadio, Ph.D
	Sophie Bastin
	Abdourahamane Konare
	Vincent O. Ajayi
Order of Authors Secondary Information:	

| Abstract: | This research work focuses on the problem of climate simulation of rainfall over West Africa and particularly over coastal countries of the Gulf of Guinea by Regional Climate Models (RCMs). The sensitivities of Weather Research and Forecasting (WRF) Model were tested for changes in horizontal resolution (convection permitting versus parameterized) on the replication of West African monsoon for year 2014. Sensitivity test was also performed for response of rainfall to changes in microphysics (MP) and planetary boundary layer (PBL) schemes. Generally, the result shows that WRF are able to replicates rainfall distribution with an adequate representation of the dynamical features of West African monsoon system. The high-resolution (wrf-4km) shows dry bias along the coast of the Gulf of Guinea but generally outperforms wrf-24km run especially in replication of the extreme rainfall distribution. The dry bias along the coastal area is suggested to not only related to convection but mostly to microphysics and PBL parameterisation schemes.
Differences were noticed between the dynamics of WRF and ERA-interim outputs despite the use of spectral nudging in the experiment which then suggest strong interactions between scales. These differences were observed to be restricted mainly to the low-layer monsoon flow in JJA. Both runs at 24km and 4km hardly simulate the typical diurnal distribution of rainfall. The sensitivity of WRF to MP (only sophisticated MP were tested) and PBL reveals a stronger impact of PBL than MP on rainfall distribution and the most significant added value over the Guinean coast and |

surroundings area was provided by the configurations using non-local PBL scheme (as ACM2). The changes in MP and PBL schemes in general seem to have less effect on the explicit runs (wrf-4km) in the replication of the rainfall over the Gulf of Guinea and the surroundings seaboard.

Revision 2

I would like to appreciate all the contribution from the reviewer to improve this work.

COMMENTS FOR THE AUTHOR:

Reviewer #1: Second review of the paper:

Does convection-permitting climate simulation improve the replication of rainfall distribution and extreme over Guinean coast and surroundings? by Kouadio et al.

First, I would like to thank the authors that addressed part of my previous recommendations. The paper is improved. Nevertheless, after a careful second read, I have some main comments that require substantial modifications. I recommend major revision before accepting this study. Please see below my main recommendations.

Comments about the previous review:

1- About the answers of the previous revision. The authors reply only to my question without any modification of the text. These questions are not for my personal interest but reveal a lack in the explanations and should imply clarification in the text. The authors must have to reconsidere some of these previous points and clarify the main document. This is, for example, for the comments L31, L326 …

- L31: what "representations" means here? forecasted? please clarify

  This question has been addressed in the first line of the abstract.

  Then, the first sentence has been modified from: "This research work focuses on the problem of representation of rainfall over West Africa and particularly over coastal countries of the Gulf of Guinea by Regional Climate Models (RCMs)." To:

  This research work focuses on the problem of climate simulation of rainfall over West Africa and particularly over coastal countries of the Gulf of Guinea by Regional Climate Models (RCMs).

- **Paragraph starting L247 and Figure 3: The authors discuss the results over the sea, but I am more curious concerning the explanations of the intense dipole E/W over the continent. This is maybe more important than over the Ocean because it affects directly the population.**

The term Guinean Coast includes all the countries around the coast. It spread till 8N. Thus, the discussion is not only about across sea but concerns the surrounding countries. The question of dipole maybe addressed in multi-years works.

The text has been modified (L284 – 305).

"This figure 3 thus shows that indeed, the run at high resolution generally, outperforms the run at 24-km resolution over the Guinean band and southern Sahel, i.e. presents an upscaled added-value. There is however, some area where the high-resolution run seems to degrade the information instead of improving the simulation, especially over Ivorian coast, south-west of Guinea and Sierra Leone. One of the main reason would be related to the fact that the better skills of the explicit run are expected at daily and sub-daily scales and for extreme values while this AV is computed over 9 months. At seasonal scale, variability is mainly driven by large-scale dynamics that is not necessary improved by the higher resolution. On the other hand, Figure 2 has shown that in comparison to TRMM and CHIRPS datasets, WRF has good performance across near-Sahel and Sahel (north of 8°N), but strongly underestimates precipitation across the coastal area of the surrounding countries of the Gulf of Guinea and mainly over the sea during the pre-onset period and at the end of the rainy season. This leads to strong dry bias from the sea to about 6N (beyond the coast) during the rainy season over Sahel. One may suggest that the introduction of this dry bias along the Gulf of Guinea seaboard toward the equator (from 5°N and equatorward) into the model simulations (either parameterized and explicit convection), may be directly related to the forcing conditions. Moreover, previous works as Meynadier et al. (2010 and Marsham et al. (2013) revealed that the southward bias in the simulation of rainfall across West Africa, is an inherent problem for RCMs. Thus, model parameterisation schemes can be point out. Furthermore, convection-permitting simulation seems not to be able to correct effectively the dry bias. Therefore, convective parameterization alone may not be enough to

explain this dry bias. Klein et al. (2015) found a similar dry bias in a cumulus, microphysics and boundary layer parameterization ensemble analysis of WRF version 3.5.1 and related it to the driving conditions."

- L268: gridded data means observed here? please clarify

The paragraph has been removed.
However, it was related to: "reliable and long-term daily observed gridded data"

- Paragraph starting L268 and Figure 4: The direct comparison between station datasets….

The section has been removed. The suggested plot can be seen in figure 5.

- Paragraph starting L316 useless and questionable, I recommend to remove it
  The section has been removed as suggested

- L324: Please clarify the reason of this specific box

This clarification can be found in the text: L213-L318;

"This box is based (1) on the availability of ground-based observation which did not spread over the whole region and also (2) to allow for better comparison of previous works as Klein et al. (2015) and those that focused on onset like Sultan and Janicot (2000, 2003)."

- L326: 25th percentile of the rainy days (conditional) or of all the days?
  The answer can be found in the text at line: L322-L324;

"It is worth noting that all the non-rain events have been beforehand removed in order to consider only the statistics based on effective rain events."

- L328: Could the authors explain how the regrid of the data can generate positive then negative changes of precipitation depending the hours of the day. It is not clear to me.

The section has been modified: L313-364

- Paragraph starting L332 is too descriptive.
  The paragraph has been adapted: L313-364

- Subsection 3.4 is also too descriptive. Please synthesize.

The section has been modified and figure changed: Subsection 3.3
- L383: The authors write "it provides more realistic estimations over the Sahel and emphasizes the benefit of the high-resolution simulation." But this is too speculative. The justifications are too few and based only on one figure that is not well adapted, and on one specific quantile.
  The graph has been adapted to support the statement section 3.3

- L394: This is too specula

The graph has been adapted to support the statement. section 3.3

- Paragraph starting L397: I recommend to remove this paragraph.
  removed previously

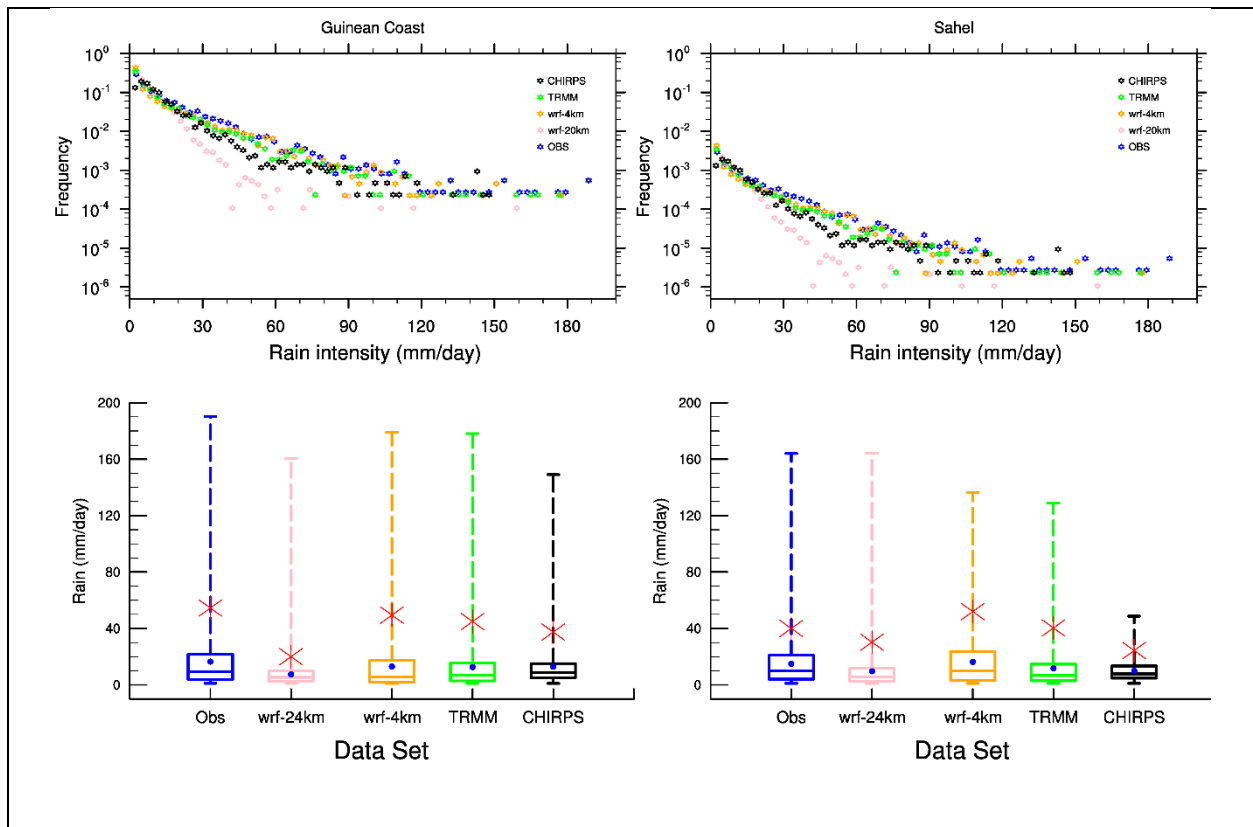- L454 Ivory Coast

Corrected: L500, L279, L280

2- About the scientific results and the impacts of the resolution. I am still convinced that most of the difference in term of precipitation values between WRF-24km and WRF-4km are explained by the size of each cells associated with each grid point (i.e. downscaling effect and not necessary a physical impact of the schemes). The authors should reconsider their methodologies to better prove these impacts. For example, what are the results of the new Fig. 5 if the authors would use the same resolution (by upscaling the WRF-4km simulation). Will they find results significantly different?

Figure 5 has been repeated with the regridded wrf-24km and wrf-4km into TRMM dataset grid scale. It is noticed from the analysis marginal differences between WRF native and regridded rainfall output at daily scale. The discussion can be found in the text at: L423-L432. The figure is added just after

Similar analysis has been made at diurnal scale (L313:L364), and the result indicate that: upscaling WRF outputs into the grid scale of TRMM dataset has an effect on the number of the events regardless of the range of rainfall intensity, however, the timing is preserved.

Thus, results may suggest a combination of both grid scale factors and physics on the observed differences between the runs at 24km (parameterized convection) and 4km (convection-permitting).

Empirical probability distribution functions of daily precipitation (top) daily. Boxplots of the daily precipitation (Bottom) respectively from the ground-based observations, wrf-24km, wrf-4km, TRMM and CHIRPS data sets over the Guinean coast (left) and the Sahelian (right) regions. The boxes indicate respectively from the bottom to the top the first, second and third interquartile ranges and the whiskers stretch to minimum and maximum values of each data set. Blue dots and the red stars represent respectively the mean value and the 95th percentile of the precipitation for each data set. Wrf-24km, wrf-4km and CHIRPS datasets have been upscale into TRMM grid scale.

This comment seems more important in this second round since the difference between the two simulations in the new Fig. 6 and 7 are not very different. By the way, are these differences significant?

3- Despite some main comments of the previous review, some figures (see details below) have a too low quality relative to the standard of this journal. The authors have to improve most of them, and should be careful with the titles, axis, captions.

Main comments on the new document:

Abstract: To me the justification of this study, and more specifically why only PBL and MP schemes are the only schemes analysed, is not well exposed. Also, the authors are still using some speculative, or at least not justified, conclusions such as 'fairly replicates', 'good simulation'. These conclusions should be better assessed with significant test. As a reminder, this study uses only one year that reduces considerably the significance of the results, the authors should be as cautious as possible.

The limitation of the study related to the specific year has been mentioned at the end of the conclusion and the abstract has been revised.

Section 3.1:

Still too long and descriptive. For example, paragraph starting L284 must be simplified.

L 293: 'Moreover, ERAI allocated shows its maximum precipitation toward the south' sounds weird to me

Paragraph L226-L239 of the previous version has been removed and the section has been modified to consider among other remarks the upscale of wrf-4km aspect.

Section 3.2:

There are some confusions when the authors discussed the quantiles of precipitation (Q95). Sometimes they are using the value of Q95 in the observation, sometimes they are using this thresholds for each dataset. Please avoid mixing up the two methods.

L349. No ERAI is not used any more in this figure, please correct.

L363: The underestimation of the model (especially with the 24-km resolution) is quite logic. That should be mentioned.

Paragraph starting L363 and Figure 5. To me, the effect of the downscaling effect of the precipitation is the main driver of the results. The authors should compare the precipitation at the same resolution.

Section 4.1 and figure 6 and 7. Could the authors check carefully what they plot and discus. In the title, caption and in the text, they mention the difference, but to me it is not. Please reconsider all this part.

At the end of the section 4.1, what are the conclusion of these difference. Do they authors consider the WRF-4 is better than WRF-24. This section is still too descriptive, general comments and main conclusions are missing.

Paragraph starting 517: To me the results are mainly explained by the resolution of each product. Please use the same resolution to fairly compared these datasets.

Empirical probability distribution functions of daily precipitation (top) daily. Boxplots of the daily precipitation (Bottom) over the Guinean coast (left) and the Sahelian (right) regions. Boxplots of the daily precipitation over the Guinean coast respectively from the ground-based observation, TRMM, ERA-interim and wrf-24km, wrf-4km from each ensemble group members of the different configurations. The boxes indicate respectively from the bottom to the top the first, second and third interquartile ranges and the whiskers stretch to minimum and maximum values of each data set. Blue dots and the red stars represent respectively the mean value and the 95 percentiles of the precipitation for each data set. Wrf-24km, wrf-4km and CHIRPS datasets have been upscale into TRMM grid scale.

Figures:

Fig 4: The quality of these figures could be improved. No need of title for each panel (this should be indicated in the caption). Legend not readable and only one is required.

The figure has been modified

Figure 5, where are the numbers mentioned at the end of the caption

Corrected

Figure 6 and 7 Difference, are you sure?

Already answer in previous comments

Figure 7 Please keep the same structure as in Fig 6 (first column ERAI, second WRF-4, third WRF-24)

The figures 6 and 7 have modified accordingly (first column ERAI, second WRF-4, third WRF-24)

Figure 9 and 10 not readable, low quality, need to be synthesized

The Figures 9 and 10 give detail information about the ensembles. It therefore going to be difficult to regroup them without missing the information. The quality of the graphs has been improved.
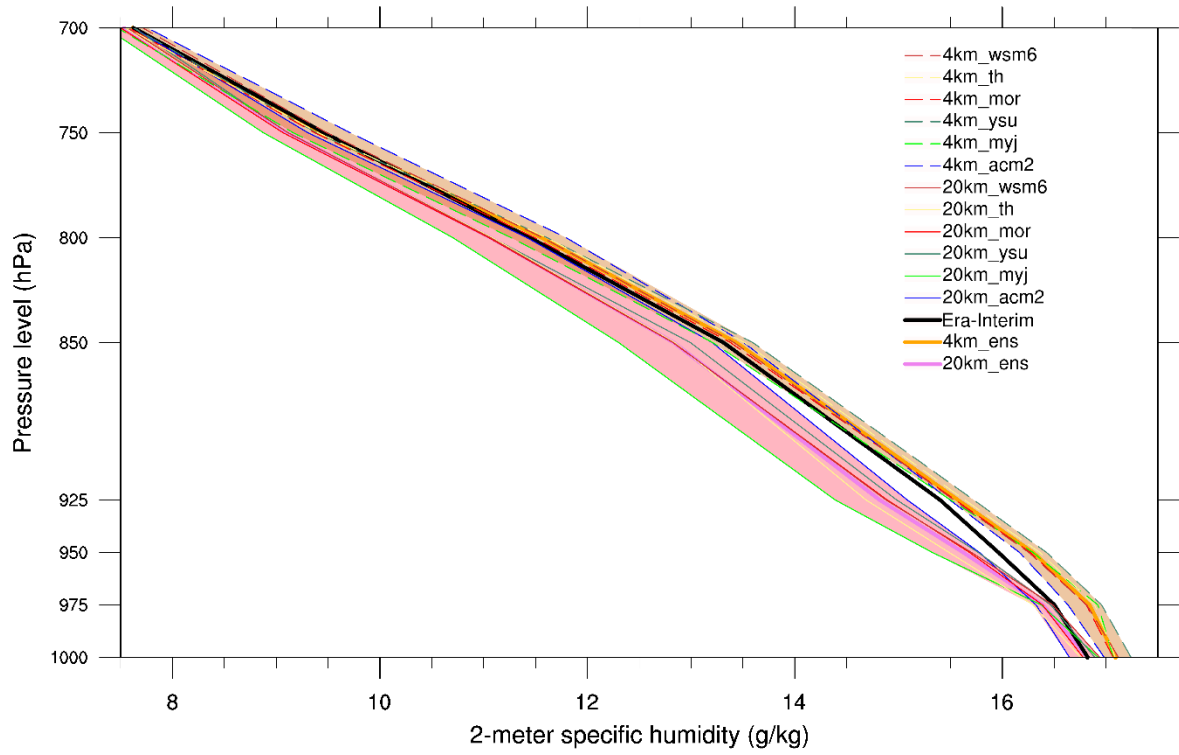
Fig. 9 Vertical profiles of specific humidity from wrf-20km and 4km sub-ensembles group members and Era-interim data set. All the values are averaged from 10W to 5E. The pink and orange coloured areas mark the range of value respectively with wrf-24km and wrf4km.
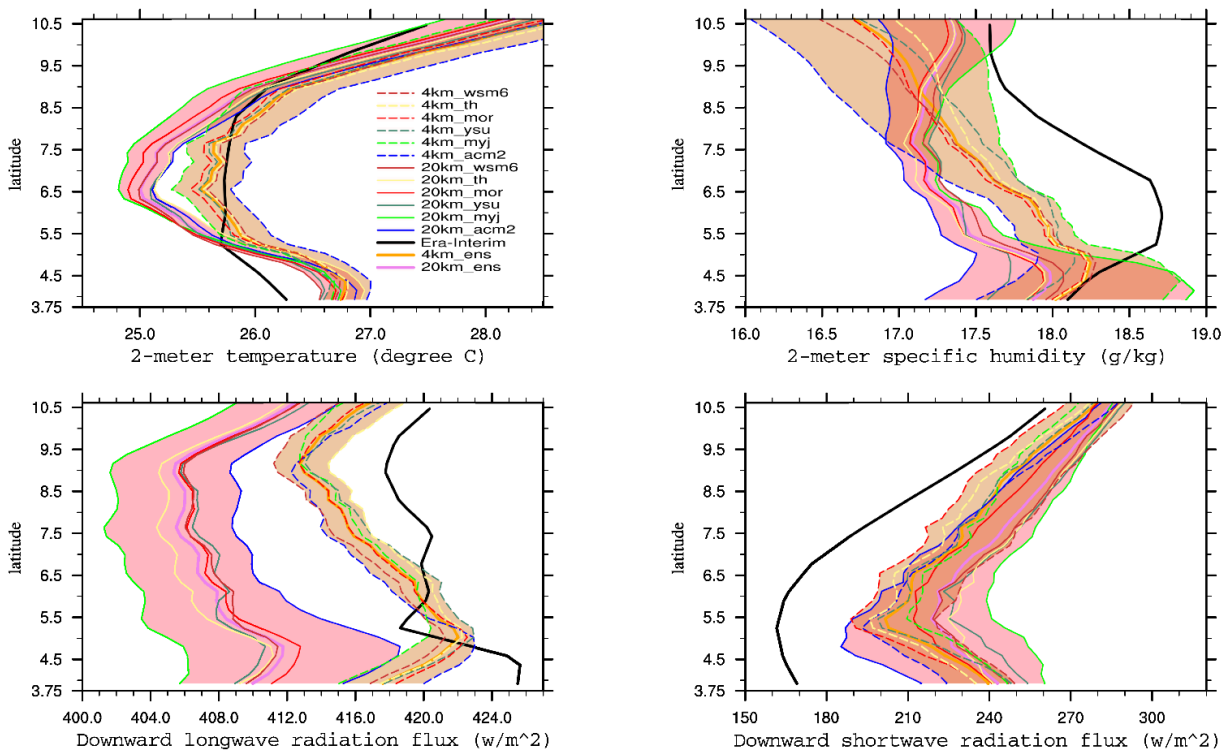
Fig. 10 Meridional evolution of 2-meter temperature, specific humidity, downward shortwave and longwave radiation fluxes from wrf-20km and 4km ensemble group members and from Era-interim data set. All the values are averaged from 10W to 5 E. The pink and orange coloured areas mark the range of value respectively with wrf-24km and wrf4km.

Figure 12 is mentioned very briefly, consider to remove it.

The figure has been removed

1   **Does convection-permitting simulate better rainfall distribution and extreme over Guinean coast**

2   **and surroundings?**

3   KOUADIO[1*], Kouakou., Sophie BASTIN[2], Abdourahamane KONARE[1]., Vincent O. AJAYI[3]

4   1- Sciences des Structures de la Matière et de Technologie (SSMT), Université Felix Houphouët-
5   Boigny, Abidjan, Côte d'Ivoire
6   2- LATMOS/IPSL, UVSQ Université Paris-Saclay, UPMC Univ. Paris 06, CNRS, Guyancourt,
7   France
8   3- WASCAL Graduate Research Program on West African Climate System (WACS)/Federal
9   University of Technology, Akure (FUTA), Nigeria

10   * Corresponding author's address :

11   Kouakou KOUADIO

12   Sciences des Structures de la Matière et de Technologie (SSMT), Université Felix Houphouët-Boigny,

13   Abidjan, Côte d'Ivoire. / 01 BP 10578 Abidjan 01

14   E-mail : kk.kouadio@yahoo.fr/

Abstract

This research work focuses on the problem of climate simulation of rainfall over West Africa and particularly over coastal countries of the Gulf of Guinea by Regional Climate Models (RCMs). The sensitivities of Weather Research and Forecasting (WRF) Model were tested for changes in horizontal resolution (convection permitting versus parameterized) on the replication of West African monsoon for year 2014. Sensitivity test was also performed for response of rainfall to changes in microphysics (MP) and planetary boundary layer (PBL) schemes. Generally, the result shows that WRF are able to replicates rainfall distribution with an adequate representation of the dynamical features of West African monsoon system. The high-resolution (wrf-4km) shows dry bias along the coast of the Gulf of Guinea but generally outperforms wrf-24km run especially in replication of the extreme rainfall distribution. The dry bias along the coastal area is suggested to not only related to convection but mostly to microphysics and PBL parameterisation schemes. Differences were noticed between the dynamics of WRF and ERA-interim outputs despite the use of spectral nudging in the experiment which then suggest strong interactions between scales. These differences were observed to be restricted mainly to the low-layer monsoon flow in JJA. Both runs at 24km and 4km hardly simulate the typical diurnal distribution of rainfall. The sensitivity of WRF to MP (only sophisticated MP were tested) and PBL reveals a stronger impact of PBL than MP on rainfall distribution and the most significant added value over the Guinean coast and surroundings area was provided by the configurations using non-local PBL scheme (as ACM2). The changes in MP and PBL schemes in general seem to have less effect on the explicit runs (wrf-4km) in the replication of the rainfall over the Gulf of Guinea and the surroundings seaboard.

2

1. Introduction

The West African region which extends from the Gulf of Guinea to the Sahel is an area which is subjected to alternating dry and wet seasons mainly linked to the monsoon, which influences the majority of annual precipitation. This region is an important source of aerosols and energy, which contributes to the formation of tropical cyclones. Therefore, this region greatly interacts with the Earth climate system and has been subject of numerous studies (Fontaine and Philippon 2000; Trenberth *et al.* 2000 ; Ali *et al.* 2005 ; Abiodun *et al.* 2008 ; Konare *et al.* 2008 ; Druyan *et al.* 2010 Moufouma-Okia and Rowell 2010 ; Sylla *et al.* 2010b ; Flaounas *et al.* 2012). West African region has also been identified as one of the poorest region in the world which depends mainly on rain-fed agriculture and one of the most vulnerable to climate change and climate variability (IPCC 2007). This vulnerability is aggravated by the interaction of 'multiple stresses' (drought frequency and duration, frequency of extreme events, among others), occurring at various levels, and the low adaptive capacity (IPCC 2007). Several studies (Omotosho et al. 2000; Sultan and Janicot 2000, 2003; Hagos and Cook 2007; Omotosho 2008; Pm. Ruti 2009; Janicot et al. 2010; Oettli et al. 2011) have argued that seasonal forecast of rainfall is crucial for socio-economic development in this sub-region. This is in the aim to (i) prevent extreme events like floods in the southern part, (ii) management of climate risk in agriculture (better preparedness for rain-fed agricultural activities), (iii) forestall outbreak of diseases in the Sahel region etc.

Although many studies have focused on the prediction of the rainfall, there exists challenges of reliable seasonal forecast due to several forcings. For example, the climate of this region is influenced by the interactions of various complex mechanisms (topography, ocean-atmosphere interactions, atmosphere-biosphere exchanges etc.). In order to address these issues, several studies investigated the patterns of inherent variability in the West African monsoon at intra-seasonal, seasonal and interannual scales with the purpose to better understand the West African Monsoon (WAM) mechanisms (Adedoyin 1989; Nicholson 2001; Brooks 2004; Okumura and Xie 2004; 2004, Steiner *et al.* 2009 ; De Coëtlogon *et al.* 2010 ; Fink *et al.* 2010 ; Gbobaniyi *et al.* 2014 ; Meynadier *et al.* 2014) and precipitation characteristics (location, intensity, duration *etc).*

The relationship between rainfall and regional or large-scale dynamics over West Africa has been reported by earlier studies (Nicholson and Grist 2003; Sultan et al. 2003). The onset of

87   the monsoon is associated with the intensification of the Tropical Easterly Jet (TEJ), a northward

88   shift and a weakening of the African Easterly Jet (AEJ), which is associated with a decrease of

89   African Easterly Waves (AEWs) activity (Lavaysse et al. 2006; Sylla et al. 2010b).   These results

90   are in agreement with observation of Omotosho (2008) which found a stronger AEJ during dry

91   years than during wet ones. Air-sea (through the Sea Surface Temperature (SST) in the Gulf of

92   Guinea) interactions also play an active role in the amount of precipitation, its spatial distribution

93   and northward migration (Leduc-Leballeur et al. 2013). (Vizy 2002) investigated the influence of

94   the Gulf of Guinea's SST anomalies (SSTAs) on the climatology of the WAM and found an

95   increase in rainfall over the Guinean coast area as a result of an increment in the lower tropospheric

96   water vapour content due to increased evaporation over the warm SSTAs. This was accompanied

97   by a decrease in rainfall over the southern Sahel. More generally, (Gaetani et al. 2017) have shown

98   that the SST warming affects the Sahelian precipitation through modifications in the global tropical

99   atmospheric dynamics, reducing the importance of the regional drivers. (Flaounas et al. 2012) and

100   (Mohino et al. 2011) also linked the onset and the different phases of precipitation over West

101   Africa to the convection over India and Indian ocean that generates Rossby waves which favors

102   the occurrence of dry air intrusion over West Africa, inhibiting convective activity. And finally,

103   the heat low dynamics has been shown to strongly influence the onset of the monsoon and its intra-

104   seasonal variability (Lavaysse et al. 2009, 2010a, b), but also its variability at longer time scales

105   due to radiative effects of water vapor that affect the regional dynamics (Evan et al. 2015). The

106   increase of CO_2 in the atmosphere also affects the precipitation at regional scale (Gaetani et al.

107   2017). An overview of the monsoon and its relationship with the climate system of the region is

108   provided by Nicholson (2013).

109   All these efforts in addition to constant progress of models are expected to allow adequate

110   representation of the WAM. However, at present day, models still have many difficulties to

111   simulate the West African climate features. Several reasons are suggested to justify these

112   underperformances ranging from the physics of the models, scale interactions, lacks of reliable

113   and dense observation data suited to the resolution of the models. For example, Chang (2011)

114   proposed that the limitation of climate models to reproduce the diurnal, seasonal and annual cycles

115   of the rainfall over West Africa is related to a limited capacity of meteorological services in getting

116   observations data set, and human and informatics resources. Indeed, the complex coupled systems

117   that modulate climate system of the region are not well incorporated in current models, and one

reason is that in most studies, precipitation is considered at monthly and regional scales, while precipitation over this area have a very strong variability when looking at higher temporal and spatial scales, with most of events occurring in the tails of classical precipitation distribution (either very intense events, either dry periods). Furthermore, Intergovernmental Panel on Climate Change (IPCC) acknowledged on its Third Assessment Report (TAR) that a model run at coarse resolution does not allow detailed extreme rainfall evaluation (Griggs and Noguer 2002). Then the simulation of the WAM at very high resolution is suggested to have a positive impact on the representation of the West African Climate, not only because the physical processes will likely be better represented but also because the explicit convection may help in the reproduction of this kind of distribution (Ban et al. 2014; Prein et al. 2015). However, some model improvements are likely necessary but the lack of observations to well define the distribution does not make the task easy.

Some earlier studies (Gallée et al. 2004; Doi et al. 2012; Holloway et al. 2012; Patricola et al. 2012; Marsham et al. 2013; Moufouma-Okia and Jones 2014; Small et al. 2014; Harlaß et al. 2017) showed an improvement of their simulations using high resolution simulation. Marsham *et al.* (2013) investigated the role of the moist convection over West Africa throughout a comparative study based on a horizontal resolution's cascade simulations using the UK Met Office Unified Model (UM). The runs are composed of grid spacing's of 4 and 12 km for 25 July to 4 August 2006. The first run is done with a convective parameterization and the second with an explicit convection. They found a better representation of the WAM with the explicit run. The major improvements come from a more realistic estimation of the latent and radiative heating in the northern part of West Africa and a better representation of the diurnal cycle of the rainfall. They noticed that these representations weaken the monsoon flow, the Sahel-Sahara pressure gradient, delaying the related diurnal cycle and modifying the interaction between monsoon and the boundary layer convection. They further reported that this result raises the importance of the interaction between monsoon and convection. In addition to the explicitly resolving of deep convection, convection-permitting run also allow a better representation of fine-scale orography and variations of surface fields. This is really important in mountainous regions and in areas with heterogeneous land surfaces like coastal and urban regions, wetlands, and patchy land covers. Therewith, resolving fine-scale surface heterogeneity is also of paramount importance due to the fact that it is an important forcing for deep convection (Prein et al. 2015).

148   However, the high-resolution simulation of the WAM remains largely under explored

149   because such type of high resolution modelling works requires high computational resources,

150   innumerable computing time, and processors to high storage capacity. As a consequence, the

151   studies conducted on the analysis of the WAM at high resolution are still too short (e.g. 11 days

152   for Marsham *et al.* (2013)) to fully make a conclusion for a model in a climate mode, when the

153   impact of the initial state will be cancelled. Therefore, the analysis of the WAM at very high

154   resolution remains an important concern. In addition, the prevention of events with high social,

155   economic and environmental impacts remains a constant challenge over the region. There is a

156   need for identification of accurate models with optimal parameterizations for better understanding

157   of the processes which allow a better prediction of West African rainfall variability and extreme

158   and then provide the best way of using of regional dynamical model as a forecast tool and

159   overcoming the difficulties of explaining the detailed rainfall and intense rainfall process over the

160   West African region and particularly along the Guinean Coast and surrounding.

161   The study presented here evaluates the added-value of performing a convective permitting

162   simulation in a climate mode, covering a longer period than a case study (several months) for the

163   representation of rainfall distribution over Guinean coast, with a focus on heavy rainfall. Several

164   combinations of parameterization schemes are compared in this explicit convective climate mode

165   and the best combinations for replication of high rainfall events over Guinean Coast and

166   surroundings are proposed. Section 2 describes the model and experiments which are compared

167   and evaluated in section 3. Section 4 assesses the role of dynamics and physics in the performance

168   of the different simulations. Finally, section 5 concludes the study.

169

170   **2. Model Description and Experiments**

171   Weather Research and Forecasting (WRF) Model is used in this study to first assess the

172   capability of High-Resolution Regional simulation (convective-permitting) of West African

173   Climate.

174   The first set of simulations uses two nested domains over the West African region (Fig.1)

175   from March to September 2014. The coarser domain extends from 25°W to 30°E and from 10°S

176   to 40°N with 24km horizontal resolution. The inner domain is one-way nested from 17°W to 10°E

6

and from 4°N to 20°N run at 4km horizontal resolution (figure 1, black rectangle). Lateral boundaries of the 24km domain are forced with Centre for Medium-Range Weather Forecasts (ECMWF) reanalyses ERA-interim (Dee et al. 2011) and it is spectrally nudged towards ERA-interim for wavelength of 1680 km in the zonal direction and of 1576 km in the meridional one to avoid unrealistic departures from the driving fields due to the size of the domain (Stauffer and Seaman 1990; Salameh et al. 2010; Omrani et al. 2012). The nudging concerns zonal and meridional wind and the temperature above the boundary layer. The configuration of WRF model includes 51 vertical layers extending up to 50 hPa, and uses the Yonsei University (YSU) planetary boundary layer scheme (Hong et al. 2006), the Noah land-surface model (Chen and Dudhia 2001), the Rapid Radiative Transfer Model for Global models (RRTMG) for shortwave (Dudhia 1989) and longwave (Mlawer et al. 1997) and the single-moment six-class (WSM6) grid-scale microphysics scheme (Hong and Lim 2006). Both domains share the same physics parameterizations except that in the nested domain, cumulus (CU) parameterization is not activated to allow explicit convection. The Kain–Fritsch (KF) convective scheme is used in the coarse domain with activation of interaction with RRTMG to take into account subgrid-scale radiative effects of clouds according to Alapaty *et al.* (2012), Herwehe *et al. (*2014).

The second set of runs is performed to focus on the physical processes of rainfall over the Guinean Coast, particularly on the influence of microphysics and boundary layer processes on the simulation of intense precipitations. These experiments consist of an ensemble of runs combining different boundary layer and microphysics schemes. Nudging is used in the coarse domain to ensure that the large-scale dynamics is the same in all the simulations of the ensemble. Table 1 provides a summary of the schemes used and the different experiments. For this second set of simulations, only one month is run (June 2014), over the domains shown by pink boxes in Fig.1. Resolutions of the two nested domains are 20 km and 4km respectively. The nested domain focuses on the southern coastal area of West Africa.

An inter-comparison of the model outputs from these different configurations versus observation data is performed to find the best configuration that may provide an optimal representation of rainfall/heavy rain over West Africa in general and particularly over the Guinean Coast area. Observations come from satellites, ground-based stations and reanalyses. The ground-based data used here are daily records of temperature and precipitation over 74 stations across West Africa where the data are available for the year 2014 and selected according to the

7

geographical position. The precipitation product from Tropical Rainfall Measuring Mission (TRMM) version 3B42V7 (3-hourly, daily) allows to cover the entire area with a 0.25° spatial resolution (Huffman *et al.* 2007). In addition to TRMM data set, the Climate Hazards Group InfraRed Precipitation with Station data (CHIRPS) rainfall dataset is used. This dataset is spanning 50°S-50°N (and all longitudes), starting in 1981 to near-present, CHIRPS incorporates 0.05° resolution satellite imagery with in-situ station data to create gridded rainfall (Funk et al. 2015).

Specific humidity and temperature at 2-m, shortwave and longwave downward radiation fluxes are also compared with ERA-Interim (at 0.75°x0.75° spatial resolution). Because of the limitation of the precipitation derived from ERAI as discussed by Di Giuseppe et al. (2013), the results with this dataset is not shown in the following graphs.

3. Evaluation of the estimated rainfall

3.1 Seasonal analysis

The simulation of rainfall by Regional Climate Model (RCM) over West Africa is still a full challenge as reported in many previous studies such as Marsham *et al.* (2013) ; Meynadier *et al.* (2014) ; Birch *et al.* (2014) and Panitz *et al.* (2014). Laprise *et al.* (2008) and Di Luca *et al.* (2012) stated that the initial concept of the nesting technique is to use RCMs like sophisticated "magnifying glasses" where ''the generated small scales accurately represent those that would be present in the driven data if they were not limited by resolution''. In this section of the work, the general improvement in the simulation of rainfall over West African region is assessed. Hereafter the terms wrf-24km and wrf-4km are used to identify respectively results from runs at 24km and 4km respectively.

The seasonal evolution of the rain belt is displayed on Figure 2 as a time-latitude diagram of 5-days run mean of precipitation averaged between 10ºW-10ºE. The date of the onset is determined here by the transitional phase when precipitation decrease over the southern area around 5°N followed by its intensification northwards as indicated by Sultan and Janicot (2000, 2003) and followed by Flaounas *et al.* (2012). It can be more or less pronounced, depending on the year.

236   The proposed oceanic phase by De Coëtlogon et al. (2010) and Leduc-Leballeur et al. (2011, 2013)

237   is shown in both TRMM and CHIRPS dataset. From April to end of May, maxima of precipitation

238   are generally located to the south 5ºN and moved to around 5ºN belt till it jumps northwards in

239   mid-July. This first phase of the monsoon latitudinal and seasonal displacement is not well

240   reproduced by both as WRF outputs estimate the maxima of rainfall over land even during spring.

241   This premature inland incursion of rainfall belt generates wet bias over land and dry bias over the

242   ocean and coastal region during spring and June. After the pre-onset period, both CHIRPS and

243   TRMM show a weakening of the rainfall in early July and it is followed by a fair recovery with a

244   maxima core around 7ºN before moving northward. Thus, July 9th can reasonably be chosen as

245   Sahelian onset date with TRMM and CHIRPS. In WRF, the monsoon rainfall belt moves

246   northwards but lower than CHIRPS and TRMM data. It is then difficult to define a day for the

247   onset with the model simulations. The farthest inland penetration is observed August 15th and this

248   is replicated by both the observational datasets and WRF simulation. It is pertinent to note that the

249   observations (especially CHIRPS) show that during this period of maximum precipitation over

250   Sahel, there is a significant precipitation events along the Guinean Coast while WRF simulation

251   replicates a dry condition. After this date, the rainfall belts retreat gradually equatorward.

252   To assess the spatial value addition of the high resolution run as again the 'coarse

253   resolution run' and both WRF simulations as against ERA-interim (not shown), we computed the

254   added value (AV) based on the equation (1) proposed by Di Luca *et al.* (2013) and modified by

255   Dosio *et al.* (2014):

256    $$AV = \frac{(X_{mod1}-X_{OBS})^2-(X_{mod2}-X_{OBS})^2}{Max((X_{mod1}-X_{OBS})^2,(X_{mod2}-X_{OBS})^2)} (1)$$

257

258 where X is the tested variable (here precipitation), the index mod1 is for the model with the coarser
259 resolution, the index mod2 for the simulation at higher resolution and OBS for Observations from
260 TRMM and CHIRPS. The AV is computed over the 9 months and all data are regridded over the
261 same grid (TRMM). Then the average value of AV for each grid point over the total period is
262 plotted on Figure 3. AV is positive where model#2's squared error is smaller than the model#1's
263 one and negative otherwise. The positive values (cool colours) suggest an improvement of
264 representation by the model#2 and the negative (warm colours) indicate where model#2 degrades
265 the information provided by the model#1. In this figure, the added value of wrf-4km to wrf-24km
266 is computed using both TRMM (top)and CHIRPS (bottom) as reference dataset. The value
267 addition of the wrf-4km as against wrf-24km which allows the evaluation of the usefulness of
268 convective-permitting run, indicates an improvement of the simulation of average rainfall using
269 the explicit run in comparison to wrf-24km in the half north of Ivory Coast, Ghana, Benin and part
270 of Nigeria. On the contrary, the area westwards of Ivory Coast towards southwards of Senegal
271 indicate that WRF-24km performs better. Above 14°N, the signal is too weak to allow a
272 conclusion. There is a very good agreement between the value added computed based on either on
273 TRMM or CHIRPS dataset.

274 This figure 3 thus shows that indeed, the run at high resolution generally, outperforms the
275 run at 24-km resolution over the Guinean band and southern Sahel, i.e. presents an upscaled added-
276 value. There is however, some area where the high-resolution run seems to degrade the information
277 instead of improving the simulation, especially over Ivorian coast, south-west of Guinea and Sierra
278 Leone. One of the main reason would be related to the fact that the better skills of the explicit run
279 are expected at daily and sub-daily scales and for extreme values while this AV is computed over
280 9 months. At seasonal scale, variability is mainly driven by large-scale dynamics that is not
281 necessary improved by the higher resolution. On the other hand, Figure 2 has shown that in
282 comparison to TRMM and CHIRPS datasets, WRF has shown result closed to the observation
283 across near-Sahel and Sahel (north of 8°N), but strongly underestimates precipitation across the
284 coastal area of the surrounding countries of the Gulf of Guinea and mainly over the sea during the
285 pre-onset period and at the end of the rainy season. This leads to strong dry bias from the sea to
286 about 6N (beyond the coast) during the rainy season over Sahel. One may suggest that the
287 introduction of this dry bias along the Gulf of Guinea seaboard toward the equator (from 5°N and
288 equatorward) into the model simulations (either parameterized and explicit convection), may be

289 directly related to the forcing conditions. Moreover, previous works as Meynadier et al. (2010 and
290 Marsham et al. (2013) revealed that the southward bias in the simulation of rainfall across West
291 Africa, is an inherent problem for RCMs. Thus, model parameterisation schemes can be point out.
292 Furthermore, convection-permitting simulation seems not to be able to correct effectively the dry
293 bias. Therefore, convective parameterization alone may not be enough to explain this dry bias.
294 Klein et al. (2015) found a similar dry bias in a cumulus, microphysics and boundary layer
295 parameterization ensemble analysis of WRF version 3.5.1 and related it to the driving conditions.
296 Here, if this dry bias could be related to a narrow north-south extent of the rain belt in WRF
297 specially in WRF-24km as discussed in Klein *et al.* (2015) it may be mostly related to the
298 microphysics and boundary layer parameterizations and not only to cumulus parameterization as
299 already suggested in Flaounas, et al. (2011) and Klein et al. (2015). This result motivated the
300 second set of runs, but this will be discussed later because we will first evaluate the impact of
301 convective-permitting simulations at higher time scales.

302 **3.2 Rainfall diurnal cycle**

303   Figure 4 shows the diurnal cycle of rainfall occurrences over the Gulf of Guinea sub region
304 for different categories of events based on their intensity. The 3-hourly average rainfall of each
305 dataset is computed over the considered region (4N-8N; 10W-10E). This box is based (1) on the
306 availability of ground-based observation which did not spread over the whole region and also (2)
307 to allow better comparison with previous works as Klein et al. (2015) and those that focused on
308 onset like Sultan and Janicot (2000, 2003). The obtained rainfall distributions have been divided
309 into three subsets according to the TRMM distribution which is considered as the reference here:
310 the light rain when the rain value is below or equal to the 25th percentile of the TRMM distribution
311 (3.46 mm/3hr), the medium rain with values between 25th and 75th (6.50 mm/3hr) percentiles, the
312 intense rain events for values above or equal the 95th percentile (9.50 mm/3hr). It is worth noting
313 that all the non-rain events have been beforehand removed in order to consider only the statistics
314 based on effective rain events. Since the resolution of the dataset can impact the number of events,
315 we computed these numbers using (1) the native grid of each dataset (solid line) and (2) the
316 regridded datasets on the TRMM grid (dashed line).

11

317   Lighter rain events occur mostly between mid-night and 12 UTC (note that local time in

318   JJA over this sub-region is close to time UTC) than during the second half of the day, with a

319   maximum of occurrence at 12 UTC according to TRMM observation dataset. Both WRF, in their

320   native grids, replicate the shape of the diurnal cycle of light rain events with a sudden decrease at

321   12 UTC, but the occurrence of events is strongly overestimated in the parameterized run. If the

322   explicit run capture well the timing of the maxima of the light rains, wrf-24km shows a 3-hours

323   early peak of light rain events. On the other hand, wrf-4km either with its native grid or the

324   regridded underestimates night lighter rain events. As of wrf-24km, the regridded data shows

325   more lighter rain events than its native data.

326   In the range of medium rain events, the diurnal cycle is of less variation in TRMM even

327   though a maximum is observed at 15 UTC and a minimum between 03 and 12 UTC. WRF-4km,

328   in its native grid spacing, shows a more pronounced peak of the maxima of medium rain events

329   and a wide rain events under the observation while its regridded product almost continuous less

330   rain events related to the native wrf-4km. However, native and regridded grid from wrf-4km

331   indicated the maxima of medium rain events at 15 UCT. Wrf-24km shows same pattern of diurnal

332   cycles of the occurrence of the medium rain events either for the native and the regridded data.

333   Nonetheless, a reduction in the number of rain events is noticed with the reggrided product. All

334   datasets agree on the timing of occurrence of minimum medium rainfall events in between 03 and

335   12 UCT. Yet, wrf-24km displays the maximum events in the interval 15 and 18 UTC.

336   According to TRMM observation data set, intense rain events can occur anytime with

337   nearly the same probability but none of the simulations reproduces this. The explicit run exhibits

338   intense rain occurrence mainly from the evening to early morning with a maximum around 00

339   UTC. The same timing of the diurnal cycle is retrieved with the regridded wrf-4km with more

340   intense rain events.

341   The relative absence of intense rain events with wrf-24km is related to the lower value of

342   the 95th percentile obtained by this convective parameterized run. The analysis of the occurrences

343   of intense rain based on the 95th percentile of wrf-24km (figure not shown) demonstrates that this

344   parameterized run mostly locates its maxima rain events in the afternoon (maximum at 15 UTC).

345   This occurrence of maxima of intense rain events at 15 UTC with the parameterized run is mainly

346   due to the fact that convection is generally high when net radiative energy is at its maximum at

347   about 15 UTC. The observed natural characteristics of rainfall are hardly replicated by models.
348   This has been earlier highlighted in previous studies and suggested to be due to parameterisation
349   of convection in the models (Marsham *et al.,* 2013, Dirmeyer *et al.,* 2012, Stephens *et al.,* 2010).
350   Wrf-4km seems to produce maximum of rain independently to the peak of the net radiative energy,
351   except for medium rain-rates. In term of diurnal mean amount and timing of rain events, wrf-4km
352   depicts results closest to the observations in comparison to wrf-24km.

353   Reggriding WRF outputs into the grid scale of TRMM dataset has an effect on the number
354   of the events regardless of the range of rainfall intensity, however, the timing is preserved.

3.3 Summary of the skill of the simulations on rainfall

356   Figure 5 shows the daily Empirical Probability Distribution Functions and the boxplots of
357   daily wrf-24km and wrf-4km precipitation compared to the ground-based observations, TRMM
358   and CHIRPS data sets. Based on the available data and the regime of the rainy season, the area has
359   been divided into two zones: the Guinean Coast (4°N-8°N and 10°W-10°E) and the Sahelian
360   region including the near Sahel (10°N-18°N and 10°W-10°E). Only the available stations of each
361   sub region are considered (CI1-7, BN1-3, GH2-5, GH7-8, GH12-62 for the Guinean Coast zone
362   and GH1, GH6, GH9-11, BF1-7, NR1-7, GH40-44 for the Sahel region). For all datasets, the
363   amount of precipitation at the nearest grid point of each station has been extracted. Following Lind
364   et al. (2016), the PDF(fig.5, top) gives a detail on the spread/intensity of the daily rainfall for each
365   of the dataset while the box plot (fig.5, bottom) for its part shows the summary of the distribution
366   of rainfall (extremes, mean state). The percentiles on the box plots have been computed by
367   considering only the wet days (the day where rainfall is above the threshold 1mm) over the period
368   March-November. For each dataset, the number of events which overpass the 95th percentile of
369   ground-based observations is also indicated. The numbers on the figure provides a clear view of
370   the ability of the model to statistically replicate intense rain events. They indicate the occurrence
371   of intense rain events with the specifics dataset.

372   Over the Guinean Coast area, there is a relative underestimation of the overall rainfall
373   tendency by both TRMM and CHIRPS estimation compared to the ground-based observations.
374   They show value generally below the ground-based observation(top). The box plots (summary)
375   show only 2.95% of rain events for TRMM and CHIRPS as intense and also 95% of the rain

13

intensities are below 39 mm/day for TRMM and ~35mm/day for CHIRPS). There are marginal differences between both satellite-based dataset as the exhibit very close frequency occurrence pattern of rainfall and similar summary in both Guinean Coast area and Sahel. Across both sub-domain (Guinea Coast and Sahel), WRF-24km shows also less intense rain events as indicated with the PDF, the small boxes and the low value of its mean rainfall amount. In Guinea Coast, 95% of the rain events are less than 21.78 mm/day and only 0.18% of the rain events are intense, while the ground-based observation shows the 95th percentile at 54.5 mm/day and a mean value of about 16.45 mm/day. The statistics displayed by the observations are well replicated by the wrf-4km, which shows 13.45 mm/day as mean value, and 4.66% of values are above the threshold of 54.4 mm/day. Thus, the explicit convection run, despite its dry bias at seasonal scale along the Guinean coastal area during the Sahelian phase of the monsoon, replicates more realistic precipitation extremes and qualitative distributions compared to the convective parametrized convection run.

Over the Sahelian region, the explicit run shows daily rainfall frequency distribution closer to TRMM, CHIRPS and the ground-based observation. The summary provides more intense rain events where 95% of the rain are up to 52.31 mm/day and the simulation runs at 24km shows less intense rain events compared to the ground-based observation. 2.95% (wrf-24km) and 11.61% (wrf-4km) of rain events are above the threshold of 40 mm/day corresponding to 95th percentile of rainfall in the Sahelian region. The numbers of rain events based on wrf-4km are 4416 in the Gulf of Guinea; and 1499 in the Sahel. This matches better those of the observation with 3683 in the Gulf of Guinea; and 1119 in the Sahel than wrf-24km which shows 8250 in the Gulf of Guinea; and 2455in the Sahel. Even though wrf-4km overestimates the number of intense rains and the intensity, it provides more realistic estimations precipitation extreme across both Guinea Coast and Sahel and emphasizes the benefit of the high-resolution simulation.

The low value of the occurrence of intense rain with wrf-24km compared to the high-resolution run may be explained by the difference of the size of the grid scale. With a coarser grid scale, there is a higher probability that sub grid scale rainfall events might not be captured. (Chen and Knutson 2008). Previous studies (Emori et al. 2005; Iorio et al. 2004; Kharin et al. 2005) which assessed climate models by using ground-based stations data concludes that it is not a simple task to make a comparison between model output and station data set. They also reported that rainfall

extreme indices might be influenced by the model resolution. The station records are essentially point estimates while the model output represents the rainfall variability over a wider spatial scales. Chen and Knutson (2008) also argued that Regional climate models are able to dynamically downscale extreme precipitation events to a spatial scale that is more comparable with observed rainfall analysis or station data. The grid scaling issues should be then reduced. Furthermore, even though it is not easy to cut off the physics from the pure resolution effect behind the differences between the runs at 24km and 4km, it nevertheless emphasizes the usefulness of running the model at higher resolution at least to focus on the extreme events. On the other hand, both rainfall from wrf-24km and wrf-4km have been upscaled to TRMM dataset grid scale to assess the impact of the downscaling effect in the differences between those two (2) WRF outputs. Similar analysis as figure 5 has been made with the reggrided data and the results (figure not shown) indicated marginal changes between the native and reggrided rainfall. For example, the comparison of the value of the 95th percentile with native and regridded shows is a reduction of about 7.41% (Gulf of Guinea) and 5.3% (Sahel) for wrf-24km while wrf-4km indicates a decrease of 7% (Gulf of Guinea) and 2.5% (Sahel). This result may suggest a combination of both grid scale factors and physics on the observed differences between the runs at 24km (parameterized convection) and 4km (convection-permitting).

4. Dynamical and physical role of the West African Monsoon

4.1 Dynamics of the monsoon and moisture flux

The link between the dynamics of the WAM and its associated rainfall has been variously investigated and emphasized the role of the atmospheric circulation and specifically the Moisture Flux Convergence (MFC) (Cook, 1999; Druyan et al., 2010 ; Fontaine et al., 2008 ; Fontaine & Philippon, 2000 ; Lebel et al., 2003 ; Nicholson, 2008, 2009, 2013 ; Nicholson et al., 2012 ; Sylla et al., 2010).

Figures 6 shows cross sections of the zonal wind from March-May (MAM), June-August (JJA) and September-November (SON) and averaged from 10°W to 10°E. The first column represents the seasonal mean, while the second and third columns represent respectively the seasonal mean bias of wrf-4km and wrf-24km related to Era-Interim. Figure 7 shows seasonal

mean of vertical profiles of the MFC, superimposed by the meridional-vertical wind vectors (v,w). For a better comparison, all data have been interpolated to the wrf-24km dataset.

The atmospheric circulations related to the WAM, characterized by the monsoon flow, the African Easterly Jet (AEJ) and the Tropical Easterly Jet (TEJ) are clearly replicated by the model outputs.

During spring (MAM), the core of the monsoon flow as shown by ERA-interim is ~ 4m.s^{-1} while WRF is showing higher monsoon flow toward the coast (wrf-24km: up to 5m/s and wrf-4km up to 3m/s) and lower flow in the north (up to 4m/s bellow for both wrf-24km and wrf-4km) (Fig. 6). Deep convection, associated with strong updrafts corresponding to the ascending branch of the Hadley cell, occurs between 6°N to 10°N and 800 hPa to 200 hPa. This feature is well reproduced by the model outputs either wrf-24km or wrf-4km (Fig. 7).

During the summer (JJA), ERA-interim shows two distinguished cores of the monsoon flow. The major one is located around 15°N and the minor one at roughly 5°N. Wrf-4km reproduces these two cores; however, the cores have the same intensity, the southern one is located further north than for ERA-interim, around 7.5°N, while the second one is around 13°N (figure not shown). The AEJ is stronger in ERA-interim than in WRF simulations, while TEJ is weaker (Fig.6). Wrf-4km is showing difference up to 1m/s while wrf-24km reaches 2m/s in term of AEJ. Both WRF output show similar replication of TEJ (up to 2m/s lower). As expected, the area of deep convection has now moved to more northerly position from its position during the spring (MAM). Both model outputs replicate this feature with more inland penetration (up to 15N) than Era- Interim (below 13N and less pronounced (Fig. 7). This inland location of the deep convection is also coherent with the distribution of rainfall with WRF. A subsidence is observed around 5°N with wrf-24km and wrf-4km while in ERA-interim, it is located further beyond the equator (around 2ºS). All these differences are coherent with the more southward position of the maximum of rainfall in ERA-interim (Figs. 2 and 3) and explain the dry bias of ERA-interim over Sahel which

459   is consistent with stronger AEJ and weaker TEJ ((Omotosho 2008)) and the dry bias of WRF above

460   the sea. Indeed, the subsidence at 5°N generates a zone of strong divergence around the coastline

461   (1000-800 hPa, 2°N-8°N) in the simulation, which is weaker and more to the south in ERA-

462   interim. Note also that just above this layer, a layer of weak convergence around 700 hPa is

463   simulated with northerly wind and likely corresponds to the low-level shallow circulation (LLSC)

464   induced by the Saharan heat low and discussed by (Zhang et al. 2006). This LLSC is not captured

465   by the reanalysis.

466   During fall (SON), the configuration is similar to the spring one with less intensity. The

467   southwesterly monsoon flow is confined southwards of 5°N with Era-Interim and stronger in WRF

468   with more inland penetration. Wrf-24km shows more intense monsoon flow with a bias up to 4-

469   5m/s and the explicit run shows bias below 3m/s relative to Era-Interim.

470   To conclude on the dynamics at seasonal and regional scales, several features can explain the

471   differences in the seasonal precipitation patterns between ERA-interim and WRF simulations,

472   despite the spectral nudging. This result reveals more or less important interactions between scales

473   over this area and an impact of regional/local processes in the dynamics of this region. Therefore,

474   the impact of physical processes seems not negligible in the representation of all elements of the

475   WAM. The differences between the two WRF domains, which share the same physics but not

476   convection, are mainly reduced to the low-level circulation, which has a stronger zonal component

477   in WRF-24km than in WRF-4km. It affects the intensity of moisture convergence between 5 and

478   10°N. Furthermore, wrf-4km shows less deviation from Era-Interim than wrf-24km in the

479   replication of the main features of the WAM. However, these differences generally less

480   pronounced or even marginal. Next section investigates the impact of physical processes by

481   performing several simulations with different physics using the same large scale forcing.

482   **4.2 Impact of physical processes**

483

484   One of the major challenge of the current Convection-Permitting Models (CPMs) are the fact

485   that they are still relying in older and traditional approach parametrization developed for

486 boundary layer turbulent in mesoscale models. Furthermore, they are running at grid spacing that
487 are not large enough to be in mesoscale model regime nor fine enough to be fallen into large-
488 scale eddy simulation regime as discussing in Tao and Moncrieff (2009)

489 4.2.1 Sensitivity of WRF parametrizations on precipitation over the southern coastal area
490

491 The aim in this section is to identify configurations that would be suitable for a better
492 representation of intense rain events over the Guinean coast area. The past conducted works like
493 Flaounas et al. (2011); Pohl et al. (2011); Klein et al. (2015), used parameterized convection. Prein
494 et al. (2015) in a review CPMs underlined the limitation of our understanding about the
495 microphysical processes and their interaction with resolved cumulus dynamics while Tao and
496 Moncrieff (2009) indicated the grid spacing issue in the representation of boundary layer turbulent.

497 The current work focuses on the sensitivity of microphysics and PBLs to the resolved cumulus and
498 contribute to the understanding of the microphysics processes and their interaction with resolved
499 cumulus dynamics. Even though, the change of the convection scheme may modify the results,
500 this will need too much resources and beyond the scope of this paper.

501 A second set of experiments has thus been performed but with smaller domains due to
502 computing resources. The inner domain has been reduced to the Guinean coast area extending
503 from the Ivory Coast to the Republic of Benin (Figure 1, pink rectangles). The period of the
504 experiment is June 2014 when many flood events have been recorded along the littoral of the Gulf
505 of Guinea and especially in Abidjan. The following different experiments use the configuration of
506 the first set except for the microphysics (MP) and planetary boundary layer (PBL) schemes, which
507 contribute to the vertical and horizontal distributions of moisture, which is a key issue in the
508 Tropics for rainfall processes ((Neelin et al. 2009); (Holloway and Neelin 2009). Nine
509 combinations of MP_PBL have been tested, using 3 different PBL schemes and 3 different MP
510 schemes. These 9 combinations are thus associated with the Kain-Fritsch convective scheme in
511 the coarser domain and with explicit convection in the inner domain. Since these parameterizations
512 manage the atmospheric moisture distribution based on the same large-scale information provided
513 by same lateral boundary conditions and the use of spectral nudging for wind and temperature, this
514 protocol is well suited to understand the role of the physical processes in the simulated rainfall
515 estimate over this specific area.

The role of the PBL scheme is to determine the flux profiles of temperature and moisture within the whole atmospheric column, hence generating tendencies that serve as input for the CU and MP schemes at every model time step. Two types of PBL schemes exist according to the way they approach the turbulence equation closure problem: local closure schemes and non-local closure schemes. In the local closure schemes approach, the turbulence fluxes at each grid point are estimated based on prognostic turbulence kinetic energy (TKE). The Mellor–Yamada–Janjic (MYJ: (Janjic 1994; Janjić 2002) boundary-layer scheme used in the first part of this paper is of this type. The non-local closure schemes consider that scale eddies are of major importance to estimate vertical mixing in the boundary layer and in the free atmosphere. The PBL YonSei University (YSU: (Hong et al. 2006)) and the Asymmetric Convective Model version 2 (ACM2: (Pleim 2007) used in this section are based on this non-local closure. Moreover, the ACM2 is a combination of local and non-local turbulence closure techniques (Xie et al. 2012).

The microphysics scheme includes all processes that control the formation of cloud droplets and ice crystals, from their growth to their fallout as precipitation. It includes explicitly-resolved water vapour, cloud and precipitation processes. The MP scheme is in charge to remove excess atmospheric moisture in case the air is still saturated, which we will refer to us as non-convective precipitation. The different MP schemes used are based on their classification of hydro-meteors. The size distributions can differ from one scheme to another. The schemes considered in this work are the single-moment six-class (WSM6) scheme (Hong and Lim, 2006), the double-moment Morrison (MOR) scheme (ten-class) (Morrison et al. 2009) and the New Thompson (TH) scheme (Thompson et al. 2008). Table 1 provides a summary of the schemes used and the different experiments.

Here attention is mostly given to the qualitative impact on rainfall over Guinean coast area. Figure 8 displays Empirical probability distribution functions of daily precipitation (top) which provides the frequency occurrence of the rain events according to the intensity and the daily boxplots of precipitation. These have been computed for wrf-24km and wrf-4km rainfall from each ensemble group members, TRMM and CHIRPS dataset across Guinea Coast area. The groups have been built using a fixed particular scheme following (Pohl et al. 2011). Thus, each ensemble group is the mean of all the configurations which use that particular scheme. The value of the rainfall is extracted at the nearest grid point of each station from the different run outputs, TRMM

546   and CHIRPS. A single time series is computed for each data set. From these time series, we

547   removed the days when observations are lacking and the dry days (where daily rainfall is below 1

548   mm/day). The result indicates significant underestimation of the overall rainfall intensity of wrf-

549   20km compared to TRMM, CHIRPS and ground-based observation as seen it with the low

550   frequency occurrence of rain events against the intensity. Wrf-4km for its part is able to retrieve a

551   good range of the rain events in regard to the intensity. CHIRPS dataset is showing statistics closer

552   to the observed ground-based data compare to TRMM which miss more rain events. The boxplot

553   of observations is then obtained from the total number of precipitating days of all stations of the

554   Guinean area (CI1-7; BN1-3, GH2-5, GH7-8, GH12-62), i.e. 586 samplings (see Tab. 2). The same

555   for TRMM and CHIRPS for which we obtained 656 and 553 samplings respectively. For the

556   simulations, the numbers of the rain events are relatively high (see Tab. 2), with lower values at

557   4km than at 20km partly due to the effect of resolution, as already explained in the previous

558   section.

559   In the month of June during which several flooding events were reported, 11.43% of events

560   above the threshold of 54.5 mm/day were recorded. All the ensemble members show less intense

561   rain events compare to the ground-based observation and TRMM data sets. In addition, the total

562   rainfall amount was also underestimated by all the ensemble members (not shown). However,

563   clearly, the main impact comes from the use of higher resolution since the mean, max, 3rd

564   interquartile and number of extreme events are always significantly higher in WRF-4km than in

565   WRF-20km ensembles.

566   The occurrence of intense rain events is about 4.21% with the ensemble with the PBL

567   scheme ACM2 which provides the closest statistics to TRMM data set, at 4km while with WRF-

568   20km run, all the ensembles do not reach at once the value of 54.5 mm/day or have an occurrence

569   below 0.3%. However, it is biased by the fact that the comparison with local rain gauges is better

570   suited to a run at 4-km resolution than at 20km resolution. Nevertheless, it appears that physics

571   also impacts the results. All statistics are in better agreement with observations than the others set

572   of runs at a similar resolution (i.e. 1st, 2nd and 3rd quartiles, mean, max and 95th percentile). It is

573   true for the domain at 20km and the one at 4-km. Two other ensembles at 4km outperform the

574   others, not for all statistics but for the value of the 95th percentile of precipitation and 3rd quartile,

575 which indicates a better ability to produce heavy rain: the ensemble using WSM6 as MP scheme
576 and the one using YSU as PBL scheme.

577 The same box plot was also performed over the Guinean Coast region (4N-8N; 10W-5E) for
578 WRF simulations and TRMM by using the same grid as TRMM before statistics are computed
579 (figure not shown). The result raised once again the better performance of the explicit convection
580 in the statistics of the rainfall distribution (moderate, intense and extreme rainfalls). This suggests
581 that the added value of the explicit run did not only come from the resolution but also from explicit
582 convection. It further emphasizes the usefulness of convection permitting in the analysis of
583 extreme rainfall and more general extreme events. However, convection permitting with high-
584 resolution run, is yet exhaustively enough to fully address the problem of simulating of rainfall
585 over West African region and especially over the Guinean Coast and surrounding.

586

587 ### 4.2.2   Impact of PBL scheme

588 Both PBLs schemes ACM2 and YSU are non-local closure schemes which gives more
589 attention to scale eddies on the estimation of vertical mixing in the boundary layer and the free
590 atmosphere. The MYJ, which is a local closure, displays less intense rain events. The better
591 performance of non-local closure schemes compared to the local one has been previously reported
592 (Pleim 2007). The non-local closure has a better ability to replicate the turbulent vertical transport
593 when both small-scale shear-driven turbulence and large-scale convective turbulence are taken
594 into account (Holtslag and Boville 1993). This also takes into account large eddy transport and
595 entrainment effects, which is essential for realistic representation of the convective boundary layer
596 and the transport of humidity from the surface to the lower free troposphere, which is key for
597 triggering of convection (Holloway and Neelin 2009). The difference of vertical profiles of
598 humidity between the six PBL sub-ensembles is shown in Fig. 9 and clearly reveals that stronger
599 differences appear between 925 and 750 hPa than close to the surface, and the moister this layer,
600 the heavier the precipitation. These differences, however, are more noticeable with wrf-20km than
601 with wrf-4km. This may suggest a less influence of the PBL scheme on the convective permitting
602 run.

603   The latitudinal evolutions of surface conditions are analysed via the latitudinal profile of

604   2-meter temperature (T2m), 2-meter specific humidity (Q2m), downward shortwave (SW) and

605   longwave (LW) radiation fluxes (Fig. 11). The analysis reveals 2 distinctive groups over the

606   Guinean Coast for T2m, Q2m, and LW, between the wrf-20km and wrf-4km. The explicit runs

607   show higher surface temperature, more humidity and more incoming longwave radiation fluxes. It

608   is also worth noting that there are important differences in the near surface humidity north of 8N.

609   While wrf-4k runs show decrease in the humidity towards the north, wrf-20km runs show an

610   increase. Important differences are also observed between the PBL ACM2 and MYJ for simulation

611   of T2m and Q2m in wrf-24km or wrf-4km runs. ACM2 PBL is warmer and drier at the surface

612   than MYJ, while the opposite is observed in the free troposphere (Fig. 10). An important difference

613   is also observed for SW but only with wrf-20km. Over the ocean, and near the coast, the spread

614   between the sub-ensembles is strong with both wrf-20km and wrf-4km. These differences over the

615   ocean likely strongly impact the humidity advection inland. Wrf-20km shows more LW with

616   ACM2 with less SW. This implies a deeper or more persistent cloud cover, despite the fact that it

617   is drier and relatively warmer on the surface. At wrf-4km runs however, there are less differences

618   between the value of SW and LW. Generally, wrf-20km simulates more SW arriving at the surface

619   than wrf-4km and vice versa for the LW.

620   4.2.3   Impact of MP scheme

621   The MP scheme is not a strong discriminant for the atmospheric specific humidity either with wrf-

622   20km and wrf-4km (Fig. 8). This is also true for T2m and Q2m (Fig 9). On the contrary, there are

623   high differences between WSM6 and MOR in the representation of the SW with wrf-4km and

624   slightly less with wrf-20km (Fig.10), and this may likely explain the differences in the rainfall

625   distribution. The vertical profiles of occurrence (%) of the Liquid Water Content (LWC) and the

626   Ice Water Content (IWC, not shown) are displayed for different bin categories in Fig. 11

627   respectively. Figure 11 shows that LWC is sensitive to the resolution more than to the MP scheme

628   used, since distributions are very similar between different MP ensembles, but very different

629   between WRF-20km and WRF-4km. At 4km, there is higher occurrence of strong values of LWC

630   between 925 and 750 hPa, consistent with higher specific humidity at this altitude. It impacts more

631   strongly LW than SW, meaning that these clouds likely appear during nighttime. For IWC,

632   differences between different MP schemes are stronger than between the two different resolutions

633   (not shown). However, the main difference exists between TH and other schemes, while the

634   difference between MOR and WSM6 is weak. It thus cannot explain the difference of SW obtained

635   between MOR and WSM6.

636

5. Conclusions

This work focuses on the sensitivity of the Weather Research and Forecasting (WRF) Model to horizontal resolution and physics schemes in the replication of West African precipitation for the year 2014. Several runs were performed with either parameterization or explicit convection. Both runs, wrf-24km and wrf-4km, at seasonal scale, are able to replicate rainfall distribution over the region. The high-resolution which uses the explicit convection exhibits driest bias along the coast of the Gulf of Guinea but generally outperforms the 24km run especially in the replication of the extreme rainfall distribution. The feature underlines the importance of high resolution on the analysis, characterization and further forecast of extreme events. At diurnal scale, based on TRMM data set, the major light rain events occur between mid-night and 12 UTC and the diurnal cycle of medium rain events has of less variation with a maximum observed at 15 UTC. Wrf-4km outperforms wrf-24km in the replication of these features especially the timing, and the number of events. Intense rain events can occur anytime with nearly the same probability but none of the simulations reproduces this. The parametrized convection run situated this maximum of occurrence of intense rain events in the afternoon at 15 UTC. This is mainly due to the fact that convection is generally high when net radiative energy is at its maximum, near 15 UTC for these regions. This has been earlier highlighted in previous studies and suggested to be intrinsic to parameterized convection (Marsham *et al.,* 2013, Dirmeyer *et al.,* 2012, Stephens *et al.,* 2010). Furthermore, the explicit run exhibits intense rain mainly from the evening to early morning with a maximum around 00 UTC, independently to the peak of the net radiative energy. In short, the observed typical diurnal distribution of the rain is hardly well simulated by the model.

The analysis also reveals an adequate representation of the dynamical features of West African monsoon system with a less subsequent added value of permitting convection in the replication of low levels atmospheric circulation. However, irrespective to the spectral nudging for wrf-24km towards ERA-interim, there are differences of the dynamical structures between ERA-interim and wrf-24km. This reveals important interactions between scales over this area and not negligible impact of regional/local processes on the dynamics of this region. Therefore, the impact of physical processes seems crucial in the representation of all elements of the WAM. Both wrf-24km and wrf-4km well replicate the seasonal evolution of the AEJ. However, they show

24

666 stronger monsoon flow and weaker AEJ compared to ERA-interim. The strong AEJ leads to
667 inhibition of the vertical ascent of moisture in ERA-interim; thus, less development of clouds. The
668 relative low value of the AEJ displayed with WRF allows the vertical ascent of the moisture
669 leading to more frequent clouds. This is in agreement with the high value of precipitation observed
670 with WRF simulations inland. On the contrary, there is a dry bias over the Gulf of Guinea and
671 surroundings seaboard (from 8°N and equatorward) with either parameterized and explicit
672 convections. This dry bias has been associated with a more northward location of the subsidence
673 branch of the Hadley cell and a less south-north spread of the rain belt observed in WRF outputs.
674 The differences between the two WRF runs, which share the same physics but not convection, are
675 mainly reduced to the low-layer monsoon flow in JJA, which has a stronger zonal component in
676 WRF-24km than in WRF-4km. It affects the intensity of moisture convergence between 5°N and
677 10°N.

678   The impact of microphysics is not as strong as that of PBL schemes in either explicit or
679 parametrized convection modes. However, some differences exist that can help in a better
680 reproduction of heavy rainfall. Note that only complex MP schemes have been tested here, and it
681 is possible that the use of more simple schemes may lead to different conclusions on the importance
682 of MP scheme. The use of a non-local PBL scheme seems critical to better transport the low-layer
683 humidity into the free troposphere and trigger convection.

684   The convection-permitting simulations thus seem well relevant to study extreme events
685 (i.e. heavy precipitation). However, the simulations can be affected by the limitation of the domain
686 size, the absence of two-way interactions between the inner domain and the rest of the globe, and
687 the lateral boundary condition issues. Thus it is still ambiguous whether RCMs actually improve
688 or degrade the larger scales information which is still a backbone for modeller and scientific
689 community in general as underlined by Laprise *et al.* (2008).

690   The upscaling of wrf-4km to TRMM grid spacing (e.g. fig.4,6 and 7) suggested that
691 differences may not be only related to grid spacing differences but a combination of both
692 physical processes and grid scale effects. This study also indicates that the grid scale impact
693 seems to be more pronounced at diurnal scale than daily and seasonal scales. In addition, as
694 suggested by Prein et al. (2015) and Tao and Moncrieff (2009), the simulation at higher
695 resolution bring out a key problem: the CPMs are still relying in the older and traditional

696   approach parameterization developed for boundary layer turbulence in mesoscale models. In the
697   other hand, the current grid spacing of CPMS are not fine enough be into eddy simulation regime
698   nor coarser to be consider as mesoscale models. This problem of upscaling is of paramount
699   importance and need to be addressed however, this is beyond the scope of the current work.

700   The current study focuses only on a specific year due to the coast of such experiment. It
701   is then important to extend to several years to allow better assessment of physical processes and
702   statistical analyses. Such work needs subsequent cluster resources and is beyond the scope of this
703   paper. The use of only three (3) microphysics and PBL and one convective parameterization
704   scheme may be a limitation of the methodology.

705   This work is a first step in performing a set of comparison of different configuration that
706   use various microphysics, PBL schemes and permitting convection. The current study justifies a
707   need for large project work which will focus on the interaction between convection resolving and
708   microphysics and PBLs schemes etc. It will contribute to better assess the skill of WRF in the
709   replication of regional and more local physical processes. Furthermore, in order to fully isolate
710   the changes related to the permitting convection from the pure grid scale impact (resolution) one
711   may need a set of experiments using explicit and parameterized convections both carried at the
712   same resolution. These are in the perspective of the Ivorian new computer center which will
713   allow such expensive experiments.

714

715

List of Tables

716 **List of Tables**

717 Table 1: Cumulus, microphysics and planetary boundary layer schemes used for the experiments

718

	PHYSICAL OPTION	REFERENCES
CUMULUS	Kain–Fritsch (KF)	(Alapaty et al. 2012)
MICROPHYSICS	Morrison double-moment (MOR)	(Morrison et al. 2009)
	New Thompson (TH)	(Thompson et al. 2008)
	WRF Single-Moment 6-class (WSM6)	Hong and Lim 2006
PLANETARY BOUNDARY LAYER	Asymmetric Convective Model V2 (ACM2)	(Pleim 2007)
	Mellor-Yamada-Janjic (MYJ)	(Janjic 1994)
	Yonsei University (YSU)	(Hong et al. 2006)

719

720

721 Table 2: Total number of rainy events over 1410 possible.

Data set	number of rain events
Observation	586
WRF_ens_acm2_20km	1312
WRF_ens_acm2_4km	665
WRF_ens_myj_20km	1238
WRF_ens_myj_4km	1001

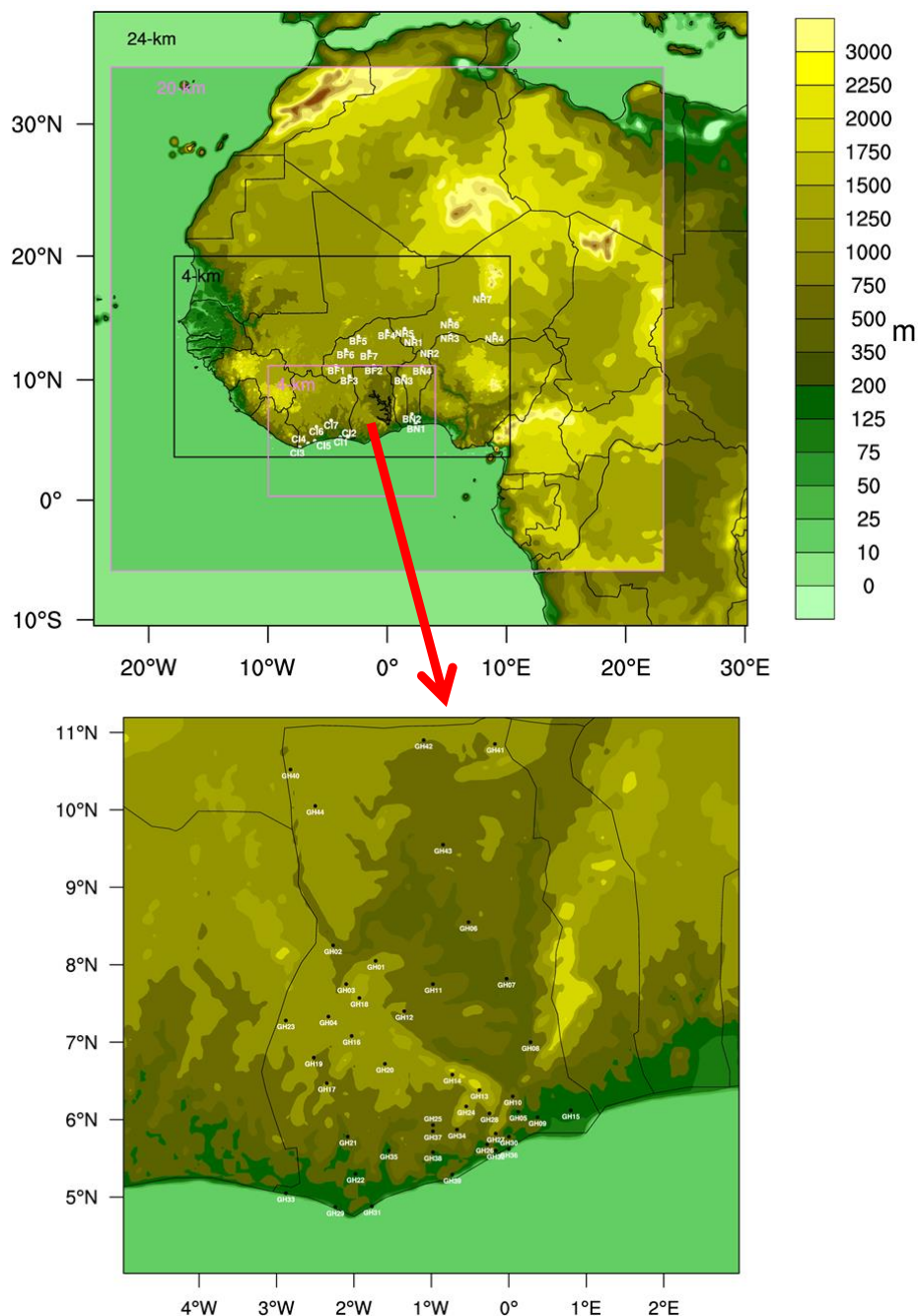|	
WRF_ens_ysu_20km	1323
WRF_ens_ysu_4km	992
WRF_ens_mor_20km	1255
WRF_ens_mor_4km	938
WRF_ens_th_20km	1340
WRF_ens_th_4km	878
WRF_ens_wsm6_20km	1321
WRF_ens_wsm6_4km	1025
WRF_ens_20km	1353
WRF_ens_4km	1070
TRMM	656
CHIRPS	553

722

723

724

725

726

727

Fig. 1 Top: WRF model domain and elevation (m); parent domain at 24 km horizontal resolution (25°W–30°E,10°S–40°N). The nested domain is depicted by the back box (17°W–10°E,4°N–20°N) black boxes (first set of runs). The pink boxes correspond to the domains for the second set of runs (sensitivity to MP and PBL schemes) where parent domain is at 20 km horizontal resolution (25°W–30°E,10°S–40°N). The nested domain covers the southern coastal area (10°W–5°E,0°N–12°N). The white dots indicate the ground-based stations used. Bottom: Zoom over Ghana (Table 1 provides the name and coordinates of the stations cited in the manuscript)
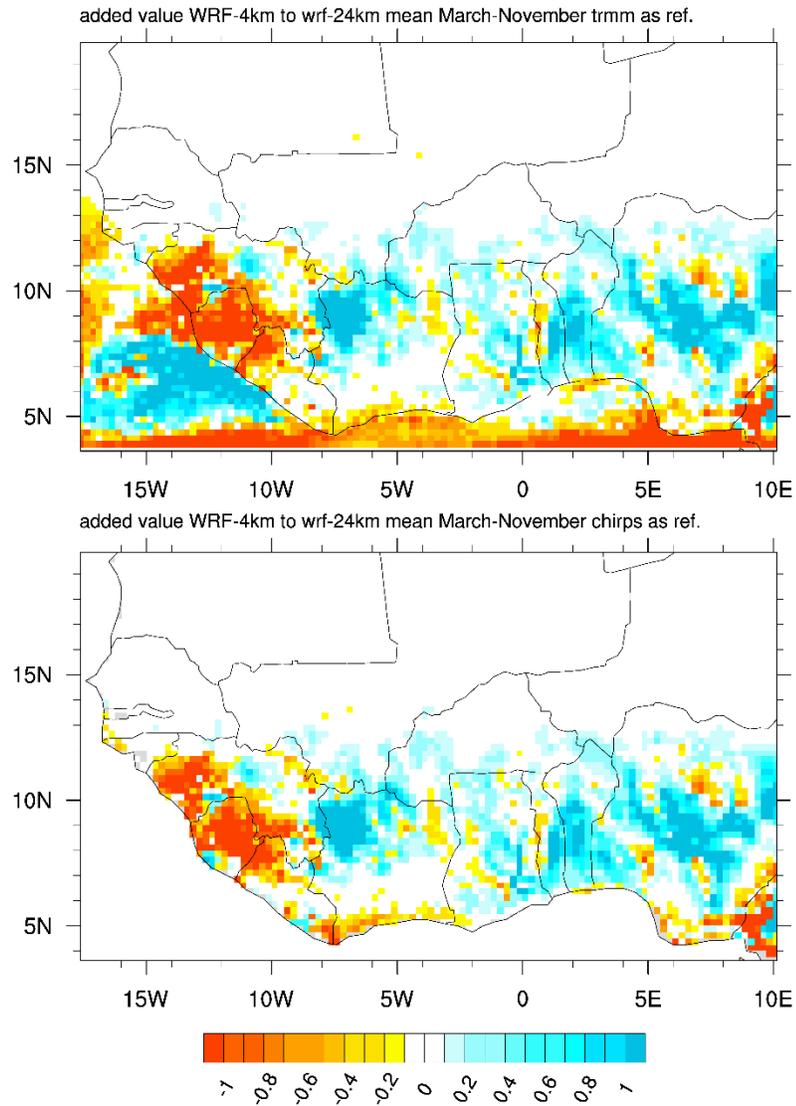
729

730

731
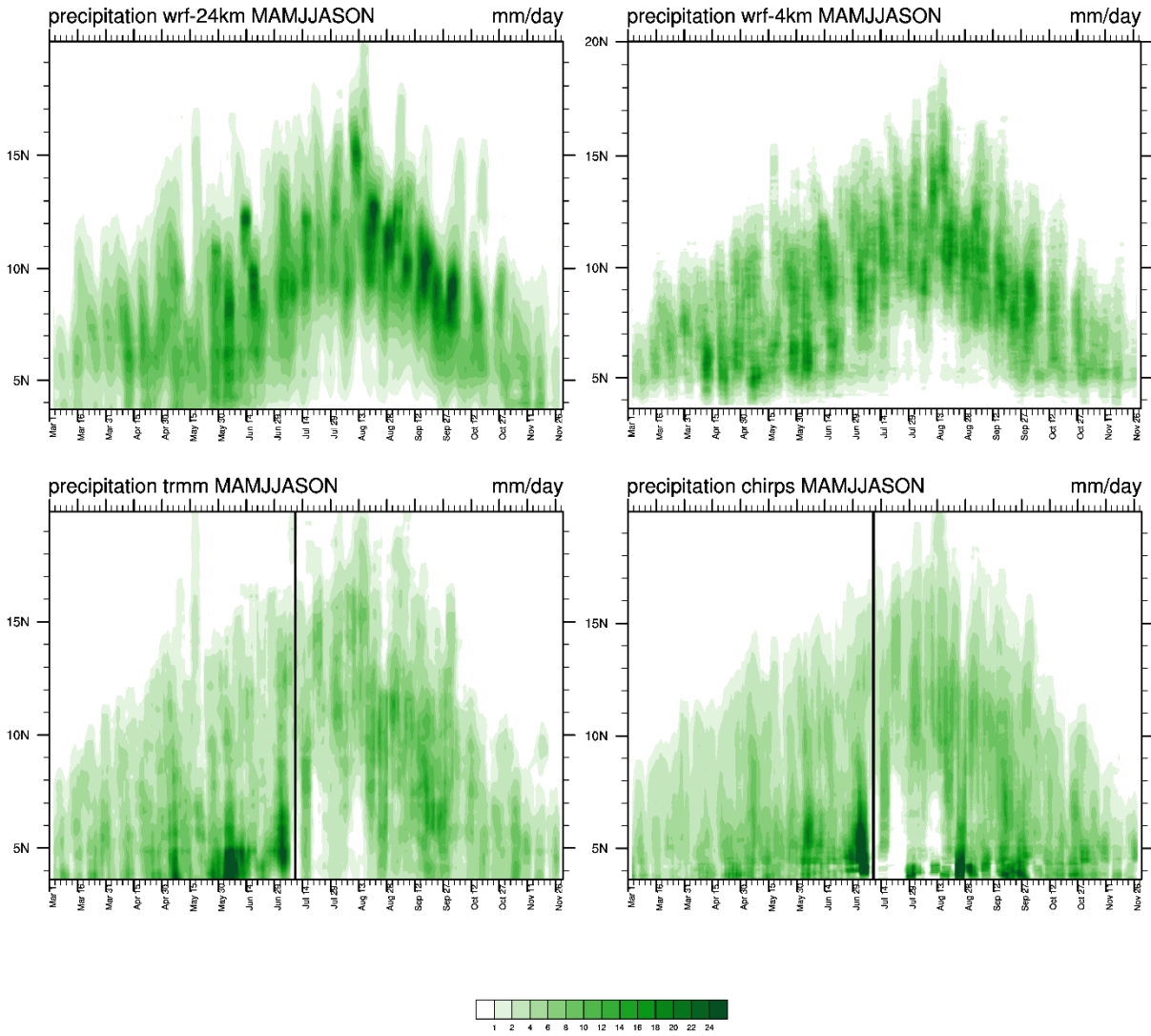
Fig. 2 Seasonal evolution (time vs. latitude) of 5-day mean precipitation averaged between 10ºW-10ºE

732

added value WRF-4km to wrf-24km mean March-November trmm as ref.

added value WRF-4km to wrf-24km mean March-November chirps as ref.

Fig. 3 Added value of high resolution (wrf-4km) simulation to coarse resolution (wrf-24km): on top computed using TRMM as reference dataset and the bottom computed using CHIRPS dataset as the reference.
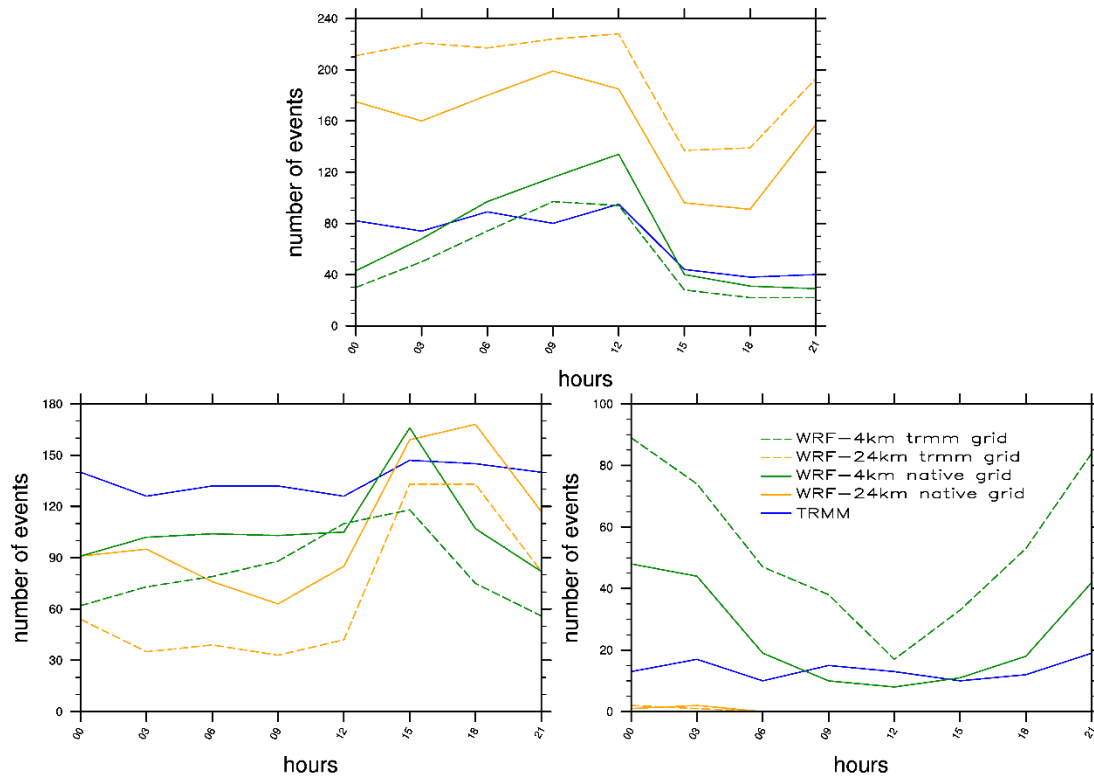
Fig. 4 Diurnal cycle of rainfall occurrence according to the range of intensity computed from TRMM distribution (light, medium, intense); from TRMM (blue), wrf-24km (orange) and wrf-4km (green), averaged over Gulf of Guinea (4°N to 8°N and 10°W to 10°E). The dotted lines account for WRF regrided into TRMM coordinates and the full lines for WRF outputs on native coordinates. Top panel shows light rainfall events; bottom-left and bottom-right present respectively the mediums and intense rainfall events.
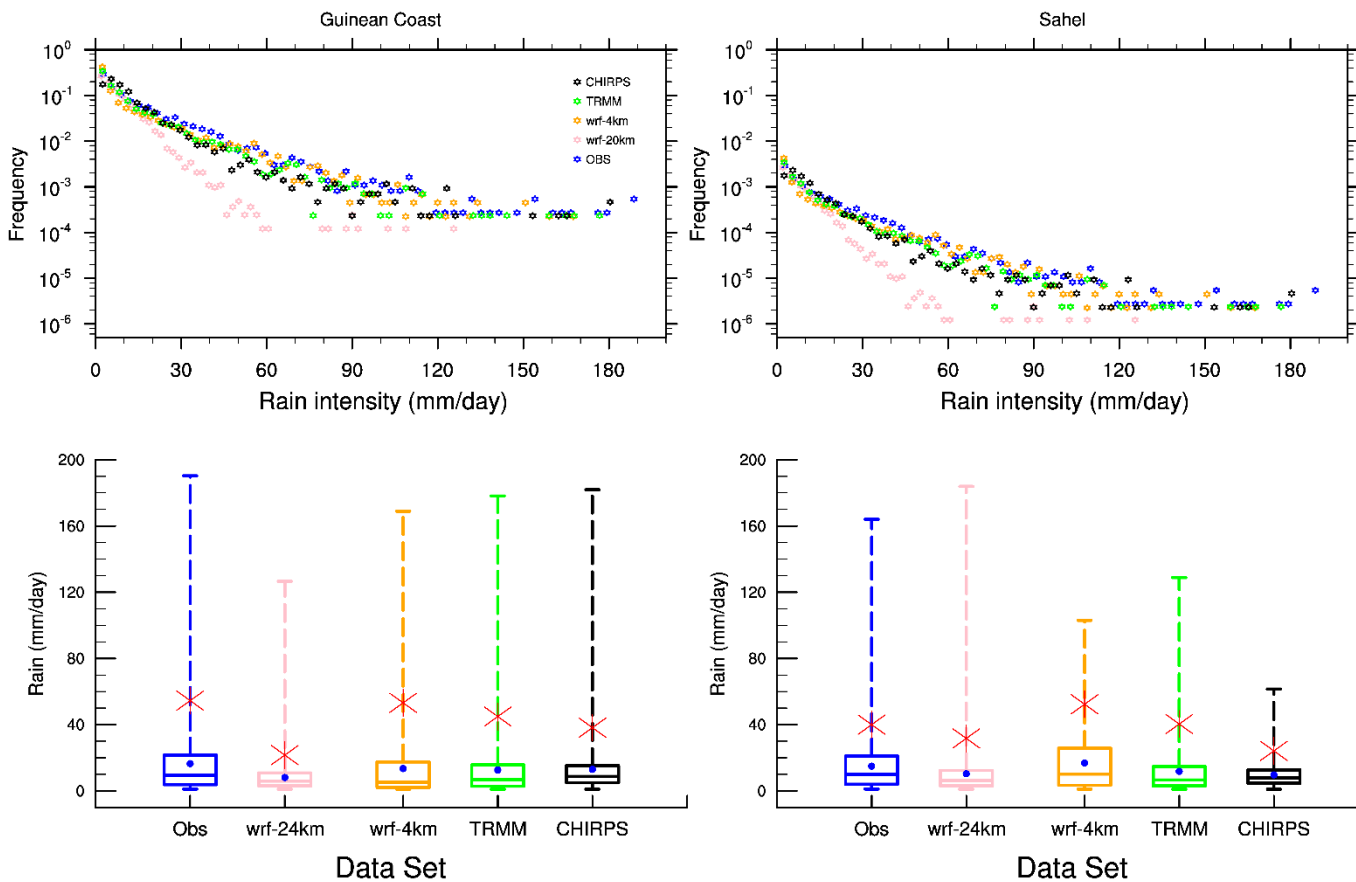
734

735

736

737

Fig. 5 Empirical probability distribution functions of daily precipitation (top) daily. Boxplots of the daily precipitation (Bottom) respectively from the ground-based observations, wrf-24km, wrf-4km, TRMM and CHIRPS data sets over the Guinean coast (left) and the Sahelian (right) regions. The boxes indicate respectively from the bottom to the top the first, second and third interquartile ranges and the whiskers stretch to minimum and maximum values of each data set. Blue dots and the red stars represent respectively the mean value and the 95th percentile of the precipitation for each data set.
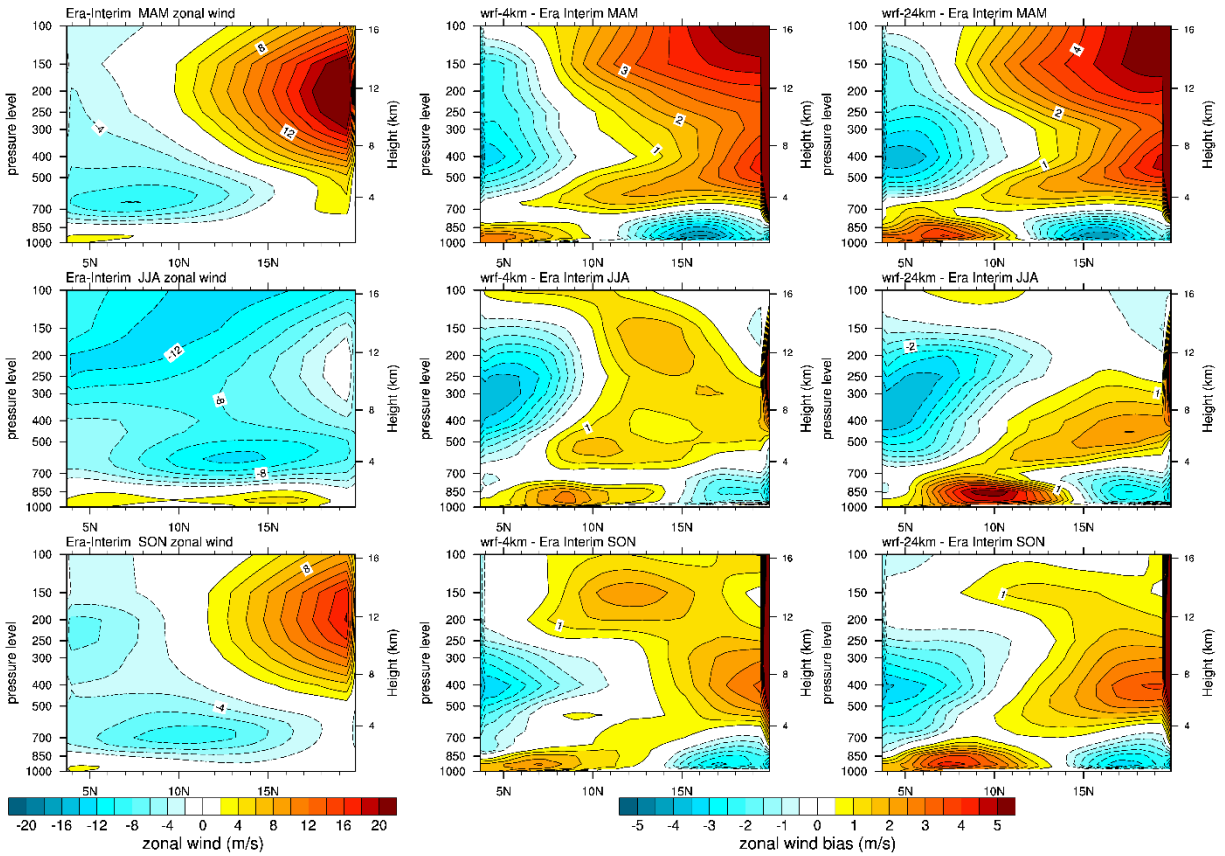
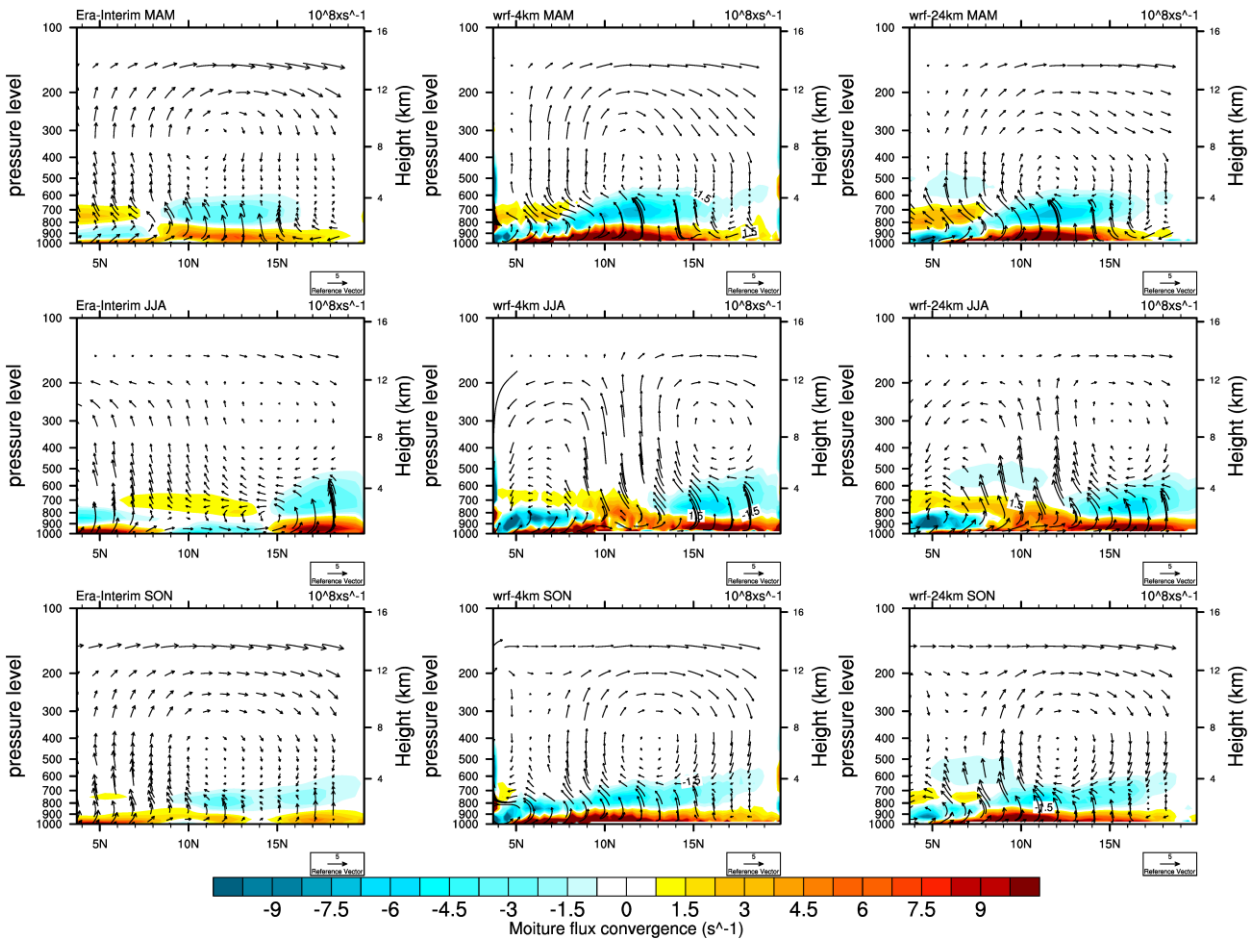**Fig. 6** Seasonal mean cross sections of the zonal wind from March-May, June-August and September-November and averaged from 10°W to 10°E. Column 1 represents ERA-interim; column 2 and column 3 represents respectively the difference between ERA-Interim, wrf-4km and wrf-24km. Dashed contours and blue colours stand for negative values and solid contours and red colours are for positive values.

742

743

Fig.7 Seasonal mean of vertical profiles of the moisture flux convergence (x $10^8 s^{-1}$, in colour) and the meridional (m/s) vertical wind vectors (x$100 Pa.s^{-1}$) (v,w). All datasets have been regridded into wrf-24km dataset, averaged for the seasons March-May, June-August and September-November and 10°W to 10°E. Column 1 represents ERA-interim; column 2 and column 3 represents respectively wrf-4km and wrf-24km.

744

745

746

Fig. 8 Empirical probability distribution functions of daily precipitation (top) daily. Boxplots of the daily precipitation (Bottom) over the Guinean coast (left) and the Sahelian (right) regions. Boxplots of the daily precipitation over the Guinean coast respectively from the ground-based observation, TRMM, ERA-interim and wrf-24km, wrf-4km from each ensemble group members of the different configurations. The boxes indicate respectively from the bottom to the top the first, second and third interquartile ranges and the whiskers stretch to minimum and maximum values of each data set. Blue dots and the red stars represent respectively the mean value and the 95 percentiles of the precipitation for each data set.

747

748
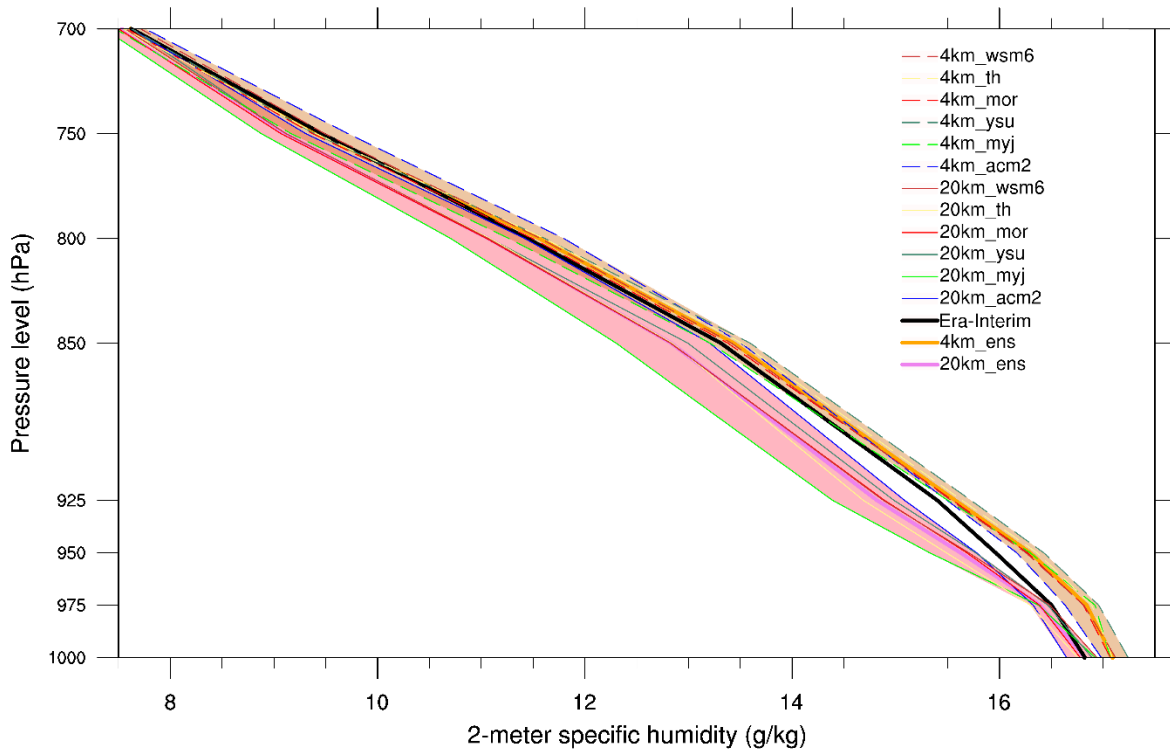
Fig. 9 Vertical profiles of specific humidity from wrf-20km and 4km sub-ensembles group members and Era-interim data set. All the values are averaged from 10W to 5E. The pink and orange coloured areas mark the range of value respectively with wrf-24km and wrf4km.

749

750

751

752

Fig. 10 Meridional evolution of 2-meter temperature, specific humidity, downward shortwave and longwave radiation fluxes from wrf-20km and 4km ensemble group members and from Era-interim data set. All the values are averaged from 10W to 5 E. The pink and orange coloured areas mark the range of value respectively with wrf-24km and wrf4km.
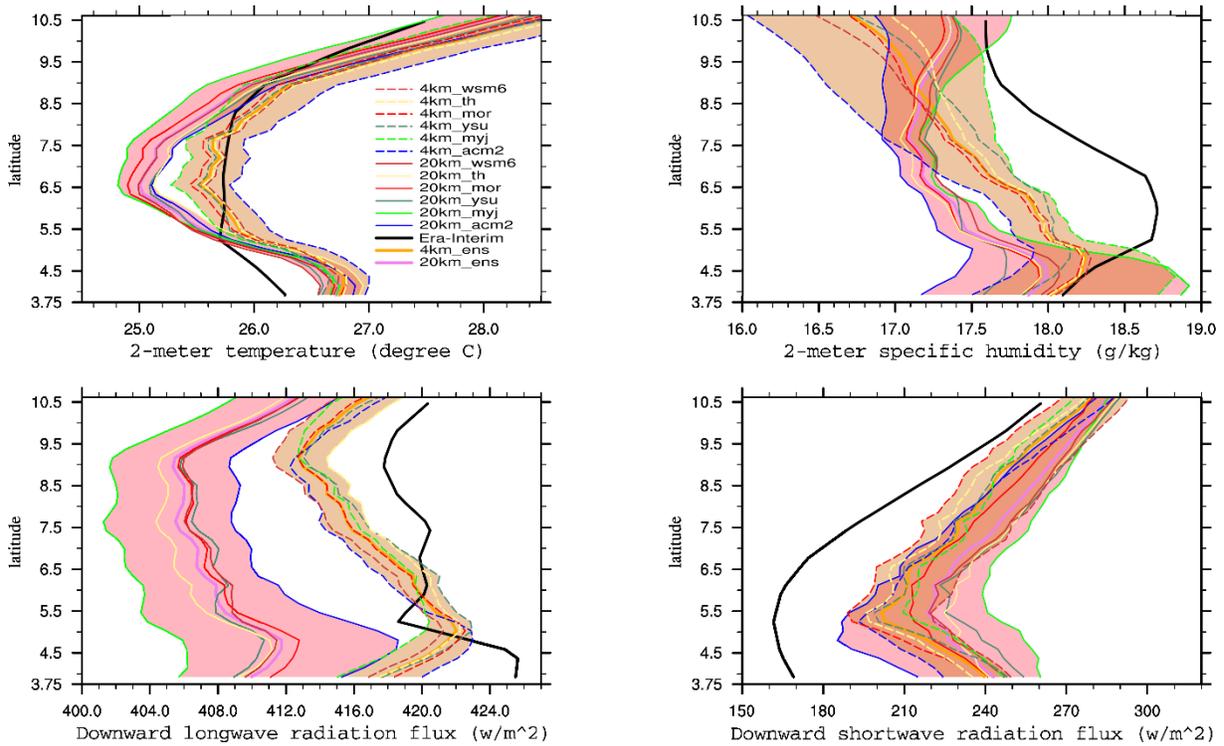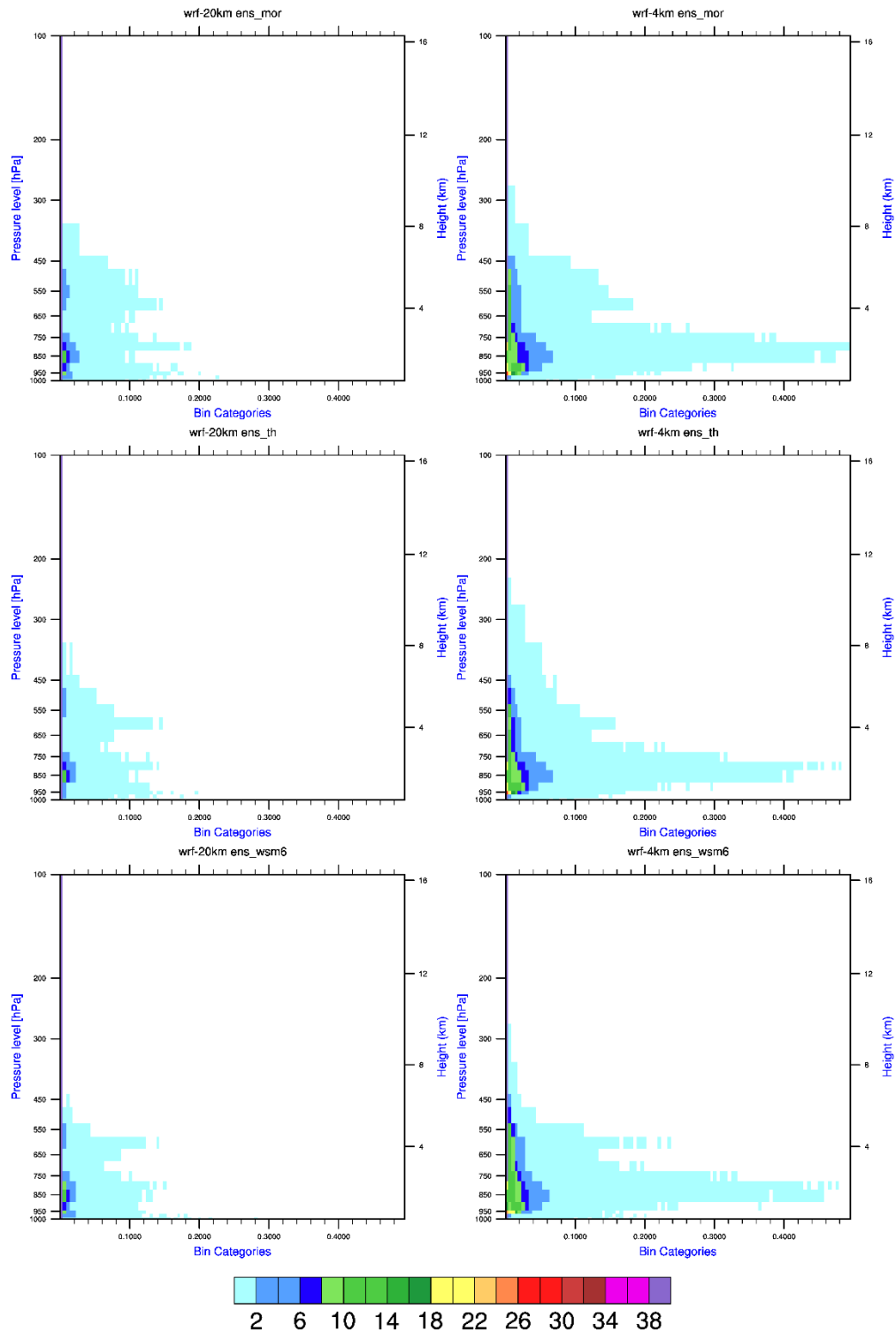
Fig. 11 Liquid Water Content from wrf-20km and 4km ensemble group members and from Era-interim data set. All the values are averaged from 10W to 5 E.

757
758

759
760
761
762 **References**

763 Abiodun BJ, Pal JS, Afiesimama EA, et al (2008) Simulation of West African monsoon using RegCM3
764   Part II: impacts of deforestation and desertification. Theor Appl Climatol 93:245–261

765 Adedoyin JA (1989) Global-scale sea-surface temperature anomalies and rainfall characteristics in
766   northern Nigeria. Int J Climatol 9:133–144

767 Alapaty K, Herwehe JA, Otte TL, et al (2012) Introducing subgrid-scale cloud feedbacks to radiation for
768   regional meteorological and climate modeling: CONVECTION AND RADIATION
769   INTERACTIONS. Geophys Res Lett 39:n/a-n/a. doi: 10.1029/2012GL054031

770 Ali A, Amani A, Diedhiou A, Lebel T (2005) Rainfall estimation in the Sahel. Part II: Evaluation of rain
771   gauge networks in the CILSS countries and objective intercomparison of rainfall products. J Appl
772   Meteorol 44:1707–1722

773 Ban N, Schmidli J, Schär C (2014) Evaluation of the convection-resolving regional climate modeling
774   approach in decade-long simulations. J Geophys Res Atmospheres 119:7889–7907

775 Birch CE, Parker DJ, Marsham JH, et al (2014) A seamless assessment of the role of convection in the
776   water cycle of the West African Monsoon. J Geophys Res Atmospheres 119:2890–2912

777 Brooks N (2004) Drought in the African Sahel: long term perspectives and future prospects. Tyndall Cent
778   Clim Change Res Norwich Work Pap 61:31

779 Chang C-P (2011) The Global Monsoon System: Research and Forecast. World Scientific

780 Chen C-T, Knutson T (2008) On the verification and comparison of extreme rainfall indices from climate
781   models. J Clim 21:1605–1621

782 Chen F, Dudhia J (2001) Coupling an advanced land surface-hydrology model with the Penn State-NCAR
783   MM5 modeling system. Part I: Model implementation and sensitivity. Mon Weather Rev
784   129:569–585

785 Coëtlogon G de, Janicot S, Lazar A (2010a) Intraseasonal variability of the ocean—atmosphere coupling
786   in the Gulf of Guinea during boreal spring and summer. Q J R Meteorol Soc 136:426–441

787 Coëtlogon G de, Janicot S, Lazar A (2010b) Intraseasonal variability of the ocean—atmosphere coupling
788   in the Gulf of Guinea during boreal spring and summer. Q J R Meteorol Soc 136:426–441

789 Cook KH (1999) Generation of the African Easterly Jet and Its Role in Determining West African
790   Precipitation. J Clim 12:1165–1184. doi: 10.1175/1520-
791   0442(1999)012<1165:GOTAEJ>2.0.CO;2

792 Dee DP, Uppala SM, Simmons AJ, et al (2011) The ERA-Interim reanalysis: configuration and
793   performance of the data assimilation system. Q J R Meteorol Soc 137:553–597. doi:
794   10.1002/qj.828

795   Di Giuseppe F, Molteni F, Dutra E (2013) Real-time correction of ERA-Interim monthly rainfall.
796   Geophys Res Lett 40:3750–3755

797   Di Luca A, de Elía R, Laprise R (2012) Potential for added value in precipitation simulated by high-
798   resolution nested regional climate models and observations. Clim Dyn 38:1229–1247

799   Di Luca A, de Elía R, Laprise R (2013) Potential for small scale added value of RCM's downscaled
800   climate change signal. Clim Dyn 40:601–618. doi: 10.1007/s00382-012-1415-z

801   Dirmeyer PA, Cash BA, Kinter III JL, et al (2012) Simulating the diurnal cycle of rainfall in global
802   climate models: Resolution versus parameterization. Clim Dyn 39:399–418

803   Doi T, Vecchi GA, Rosati AJ, Delworth TL (2012) Biases in the Atlantic ITCZ in seasonal–interannual
804   variations for a coarse-and a high-resolution coupled climate model. J Clim 25:5494–5511

805   Dosio A, Panitz H-J, Schubert-Frisius M, Lüthi D (2014) Dynamical downscaling of CMIP5 global
806   circulation models over CORDEX-Africa with COSMO-CLM: evaluation over the present
807   climate and analysis of the added value. Clim Dyn 44:2637–2661. doi: 10.1007/s00382-014-
808   2262-x

809   Druyan LM, Feng J, Cook KH, et al (2010) The WAMME regional model intercomparison study. Clim
810   Dyn 35:175–192. doi: 10.1007/s00382-009-0676-7

811   Dudhia J (1989) Numerical study of convection observed during the winter monsoon experiment using a
812   mesoscale two-dimensional model. J Atmospheric Sci 46:3077–3107

813   Emori S, Hasegawa A, Suzuki T, Dairaku K (2005) Validation, parameterization dependence, and future
814   projection of daily precipitation simulated with a high-resolution atmospheric GCM. Geophys
815   Res Lett 32:

816   Evan AT, Flamant C, Lavaysse C, et al (2015) Water vapor–forced greenhouse warming over the Sahara
817   Desert and the recent recovery from the Sahelian drought. J Clim 28:108–123

818   Fink AH, Schrage JM, Kotthaus S (2010) On the potential causes of the nonstationary correlations
819   between West African precipitation and Atlantic hurricane activity. J Clim 23:5437–5456

820   Flaounas E, Bastin S, Janicot S (2011) Regional climate modelling of the 2006 West African monsoon:
821   sensitivity to convection and planetary boundary layer parameterisation using WRF. Clim Dyn
822   36:1083–1105

823   Flaounas E, Janicot S, Bastin S, Roca R (2012) The West African monsoon onset in 2006: sensitivity to
824   surface albedo, orography, SST and synoptic scale dry-air intrusions using WRF. Clim Dyn
825   38:685–708

826   Fontaine B, Louvet S, Roucou P (2008) Definition and predictability of an OLR based West African
827   monsoon onset. Int J Climatol 28:1097–1798

828   Fontaine B, Philippon N (2000) Seasonal evolution of boundary layer heat content in the West African
829   monsoon from the NCEP/NCAR reanalysis (1968–1998). Int J Climatol 20:1777–1790

830   Funk C, Peterson P, Landsfeld M, et al (2015) The climate hazards infrared precipitation with stations—a
831   new environmental record for monitoring extremes. Sci Data 2:150066

832   Gaetani M, Flamant C, Bastin S, et al (2017) West African monsoon dynamics and precipitation: the
833   competition between global SST warming and CO2 increase in CMIP5 idealized simulations.
834   Clim Dyn 48:1353–1373

835   Gallée H, Moufouma-Okia W, Bechtold P, et al (2004) A high-resolution simulation of a West African
836   rainy season using a regional climate model. J Geophys Res Atmospheres 109:D05108. doi:
837   10.1029/2003JD004020

838   Gbobaniyi E, Sarr A, Sylla MB, et al (2014) Climatology, annual cycle and interannual variability of
839   precipitation and temperature in CORDEX simulations over West Africa. Int J Climatol 34:2241–
840   2257

841   Griggs DJ, Noguer M (2002) Climate change 2001: the scientific basis. Contribution of working group I
842   to the third assessment report of the intergovernmental panel on climate change. Weather 57:267–
843   269

844   Grist JP, Nicholson SE (2001) A study of the dynamic factors influencing the rainfall variability in the
845   West African Sahel. J Clim 14:1337–1359

846   Hagos SM, Cook KH (2007) Dynamics of the West African Monsoon Jump. J Clim 20:5264–5284. doi:
847   10.1175/2007JCLI1533.1

848   Harlaß J, Latif M, Park W (2017) Alleviating tropical Atlantic sector biases in the Kiel climate model by
849   enhancing horizontal and vertical atmosphere model resolution: climatology and interannual
850   variability. Clim Dyn 1–31

851   Herwehe JA, Alapaty K, Spero TL, Nolte CG (2014) Increasing the credibility of regional climate
852   simulations by introducing subgrid-scale cloud-radiation interactions: RCM sims with Cu-
853   radiation interactions. J Geophys Res Atmospheres 119:5317–5330. doi: 10.1002/2014JD021504

854   Holloway CE, Neelin JD (2009) Moisture vertical structure, column water vapor, and tropical deep
855   convection. J Atmospheric Sci 66:1665–1683

856   Holloway CE, Woolnough SJ, Lister GMS (2012) Precipitation distributions for explicit versus
857   parametrized convection in a large-domain high-resolution tropical case study. Q J R Meteorol
858   Soc 138:1692–1708

859   Holtslag AAM, Boville BA (1993) Local versus nonlocal boundary-layer diffusion in a global climate
860   model. J Clim 6:1825–1842

861   Hong S-Y, Lim J-OJ (2006) The WRF single-moment 6-class microphysics scheme (WSM6). J Korean
862   Meteor Soc 42:129–151

863   Hong S-Y, Noh Y, Dudhia J (2006) A new vertical diffusion package with an explicit treatment of
864   entrainment processes. Mon Weather Rev 134:2318–2341

865 Huffman GJ, Bolvin DT, Nelkin EJ, et al (2007) The TRMM Multisatellite Precipitation Analysis
866   (TMPA): Quasi-Global, Multiyear, Combined-Sensor Precipitation Estimates at Fine Scales. J
867   Hydrometeorol 8:38–55. doi: 10.1175/JHM560.1

868 Iorio JP, Duffy PB, Govindasamy B, et al (2004) Effects of model resolution and subgrid-scale physics on
869   the simulation of precipitation in the continental United States. Clim Dyn 23:243–258

870 Janicot S, Mounier F, Gervois S, et al (2010) The dynamics of the West African monsoon. Part V: The
871   detection and role of the dominant modes of convectively coupled equatorial Rossby waves. J
872   Clim 23:4005–4024

873 Janjic ZI (1994) The step-mountain eta coordinate model: Further developments of the convection,
874   viscous sublayer, and turbulence closure schemes. Mon Weather Rev 122:927–945

875 Janjić ZI (2002) Nonsingular implementation of the Mellor–Yamada level 2.5 scheme in the NCEP Meso
876   model. NCEP Off Note 437:61

877 Kharin VV, Zwiers FW, Zhang X (2005) Intercomparison of near-surface temperature and precipitation
878   extremes in AMIP-2 simulations, reanalyses, and observations. J Clim 18:5201–5223

879 Klein C, Heinzeller D, Bliefernicht J, Kunstmann H (2015) Variability of West African monsoon patterns
880   generated by a WRF multi-physics ensemble. Clim Dyn 1–23

881 Konare A, Zakey AS, Solmon F, et al (2008) A regional climate modeling study of the effect of desert
882   dust on the West African monsoon. J Geophys Res 113:. doi: 10.1029/2007JD009322

883 Laprise R, De Elia R, Caya D, et al (2008) Challenging some tenets of regional climate modelling.
884   Meteorol Atmospheric Phys 100:3–22

885 Lavaysse C, Diedhiou A, Laurent H, Lebel T (2006) African Easterly Waves and convective activity in
886   wet and dry sequences of the West African Monsoon. Clim Dyn 27:319–332

887 Lavaysse C, Flamant C, Janicot S, et al (2009) Seasonal evolution of the West African heat low: a
888   climatological perspective. Clim Dyn 33:313–330. doi: 10.1007/s00382-009-0553-4

889 Lavaysse C, Flamant C, Janicot S (2010a) Regional-scale convection patterns during strong and weak
890   phases of the Saharan heat low. Atmospheric Sci Lett 11:255–264

891 Lavaysse C, Flamant C, Janicot S, Knippertz P (2010b) Links between African easterly waves,
892   midlatitude circulation and intraseasonal pulsations of the West African heat low. Q J R Meteorol
893   Soc 136:141–158

894 Lebel T, Diedhiou A, Laurent H (2003) Seasonal cycle and interannual variability of the Sahelian rainfall
895   at hydrological scales. J Geophys Res Atmospheres 1984–2012 108:

896 Leduc-Leballeur M, De Coëtlogon G, Eymard L (2013) Air–sea interaction in the Gulf of Guinea at
897   intraseasonal time-scales: wind bursts and coastal precipitation in boreal spring. Q J R Meteorol
898   Soc 139:387–400

899 Leduc-Leballeur M, Eymard L, De Coëtlogon G (2011) Observation of the marine atmospheric boundary
900   layer in the Gulf of Guinea during the 2006 boreal spring. Q J R Meteorol Soc 137:992–1003

901 Lind P, Lindstedt D, Kjellström E, Jones C (2016) Spatial and Temporal Characteristics of Summer
902   Precipitation over Central Europe in a Suite of High-Resolution Climate Models. J Clim
903   29:3501–3518. doi: 10.1175/JCLI-D-15-0463.1

904 Marsham JH, Dixon NS, Garcia-Carreras L, et al (2013) The role of moist convection in the West African
905   monsoon system: Insights from continental-scale convection-permitting simulations. Geophys
906   Res Lett 40:1843–1849

907 Meynadier R, Bock O, Gervois S, et al (2010) West African Monsoon water cycle: 2. Assessment of
908   numerical weather prediction water budgets. J Geophys Res Atmospheres 1984–2012 115:

909 Meynadier R, De Coëtlogon G, Bastin S, et al (2014) Sensitivity testing of WRF parameterizations on
910   air–sea interaction and its impact on water cycle in the Gulf of Guinea. Q J R Meteorol Soc

911 Mlawer EJ, Taubman SJ, Brown PD, et al (1997) Radiative transfer for inhomogeneous atmospheres:
912   RRTM, a validated correlated-k model for the longwave. J Geophys Res Atmospheres 1984–2012
913   102:16663–16682

914 Mohino E, Rodríguez-Fonseca B, Mechoso CR, et al (2011) Impacts of the tropical Pacific/Indian Oceans
915   on the seasonal cycle of the West African monsoon. J Clim 24:3878–3891

916 Morrison H, Thompson G, Tatarskii V (2009) Impact of cloud microphysics on the development of
917   trailing stratiform precipitation in a simulated squall line: Comparison of one-and two-moment
918   schemes. Mon Weather Rev 137:991–1007

919 Moufouma-Okia W, Jones R (2014) Resolution dependence in simulating the African hydroclimate with
920   the HadGEM3-RA regional climate model. Clim Dyn 1–24

921 Moufouma-Okia W, Rowell DP (2010) Impact of soil moisture initialisation and lateral boundary
922   conditions on regional climate model simulations of the West African Monsoon. Clim Dyn
923   35:213–229

924 Neelin JD, Peters O, Hales K (2009) The Transition to Strong Convection. J Atmospheric Sci 66:2367–
925   2384. doi: 10.1175/2009JAS2962.1

926 Nicholson SE (2001) Climatic and environmental change in Africa during the last two centuries. Clim
927   Res 17:123–144

928 Nicholson SE (2013a) The West African Sahel: A review of recent studies on the rainfall regime and its
929   interannual variability. ISRN Meteorol 2013:

930 Nicholson SE (2013b) The West African Sahel: A review of recent studies on the rainfall regime and its
931   interannual variability. ISRN Meteorol 2013:

932 Nicholson SE (2008) The intensity, location and structure of the tropical rainbelt over west Africa as
933   factors in interannual variability. Int J Climatol 28:1775–1785. doi: 10.1002/joc.1507

934 Nicholson SE (2009) A revised picture of the structure of the "monsoon" and land ITCZ over West
935   Africa. Clim Dyn 32:1155–1171

936 Nicholson SE (2013c) The West African Sahel: A review of recent studies on the rainfall regime and its
937   interannual variability. ISRN Meteorol 2013:

938 Nicholson SE, Dezfuli AK, Klotter D (2012) A two-century precipitation dataset for the continent of
939   Africa. Bull Am Meteorol Soc 93:1219–1231

940 Nicholson SE, Grist JP (2003) The seasonal evolution of the atmospheric circulation over West Africa
941   and equatorial Africa. J Clim 16:1013–1030

942 Oettli P, Sultan B, Baron C, Vrac M (2011) Are regional climate models relevant for crop yield prediction
943   in West Africa? Environ Res Lett 6:14008

944 Okumura Y, Xie S-P (2004) Interaction of the Atlantic Equatorial Cold Tongue and the African
945   Monsoon*. J Clim 17:3589–3602

946 Omotosho JB (2008) Pre-rainy season moisture build-up and storm precipitation delivery in the West
947   African Sahel. Int J Climatol 28:937–946. doi: 10.1002/joc.1548

948 Omotosho JB, Balogun AA, Ogunjobi K, others (2000) Predicting monthly and seasonal rainfall, onset
949   and cessation of the rainy season in West Africa using only surface data. Int J Climatol 20:865–
950   880

951 Omrani H, Drobinski P, Dubos T (2012) Spectral nudging in regional climate modelling: how strongly
952   should we nudge? Q J R Meteorol Soc 138:1808–1813

953 Panitz H-J, Dosio A, Büchner M, et al (2014) COSMO-CLM (CCLM) climate simulations over
954   CORDEX-Africa domain: analysis of the ERA-Interim driven simulations at 0.44 and 0.22
955   resolution. Clim Dyn 42:3015–3038

956 Patricola CM, Li M, Xu Z, et al (2012) An investigation of tropical Atlantic bias in a high-resolution
957   coupled regional climate model. Clim Dyn 39:2443–2463

958 Pleim JE (2007) A combined local and nonlocal closure model for the atmospheric boundary layer. Part
959   II: Application and evaluation in a mesoscale meteorological model. J Appl Meteorol Climatol
960   46:1396–1409

961 Pm. Ruti AD (2009) How do the large-scale models represent the West African intra-seasonal variability
962   and its relationship with remote or local forcing

963 Pohl B, Crétat J, Camberlin P (2011) Testing WRF capability in simulating the atmospheric water cycle
964   over Equatorial East Africa. Clim Dyn 37:1357–1379

965 Prein AF, Langhans W, Fosser G, et al (2015) A review on regional convection-permitting climate
966   modeling: Demonstrations, prospects, and challenges. Rev Geophys 53:323–361

967 Salameh T, Drobinski P, Dubos T (2010) The effect of indiscriminate nudging time on large and small
968   scales in regional climate modelling: application to the Mediterranean basin. Q J R Meteorol Soc
969   136:170–182

970 Small RJ, Bacmeister J, Bailey D, et al (2014) A new synoptic scale resolving global climate simulation
971   using the Community Earth System Model. J Adv Model Earth Syst 6:1065–1094

972 Stauffer DR, Seaman NL (1990) Use of four-dimensional data assimilation in a limited-area mesoscale
973   model. Part I: Experiments with synoptic-scale data. Mon Weather Rev 118:1250–1277

974 Steiner AL, Pal JS, Rauscher SA, et al (2009) Land surface coupling in regional climate simulations of
975   the West African monsoon. Clim Dyn 33:869–892

976 Stephens GL, L'Ecuyer T, Forbes R, et al (2010) Dreary state of precipitation in global models. J
977   Geophys Res Atmospheres 115:

978 Sultan B, Janicot S (2000) Abrupt shift of the ITCZ over West Africa and intra-seasonal variability.
979   Geophys Res Lett 27:3353–3356

980 Sultan B, Janicot S (2003) The West African monsoon dynamics. Part II: The "preonset" and "onset" of
981   the summer monsoon. J Clim 16:3407–3427

982 Sultan B, Janicot S, Diedhiou A (2003) The West African monsoon dynamics. Part I: Documentation of
983   intraseasonal variability. J Clim 16:3389–3406

984 Sylla MB, Coppola E, Mariotti L, et al (2010a) Multiyear simulation of the African climate using a
985   regional climate model (RegCM3) with the high resolution ERA-interim reanalysis. Clim Dyn
986   35:231–247

987 Sylla MB, Dell'Aquila A, Ruti PM, Giorgi F (2010b) Simulation of the intraseasonal and the interannual
988   variability of rainfall over West Africa with RegCM3 during the monsoon period. Int J Climatol
989   30:1865–1883

990 Tao W-K, Moncrieff MW (2009) Multiscale cloud system modeling. Rev Geophys 47:

991 Thompson G, Field PR, Rasmussen RM, Hall WD (2008) Explicit forecasts of winter precipitation using
992   an improved bulk microphysics scheme. Part II: Implementation of a new snow parameterization.
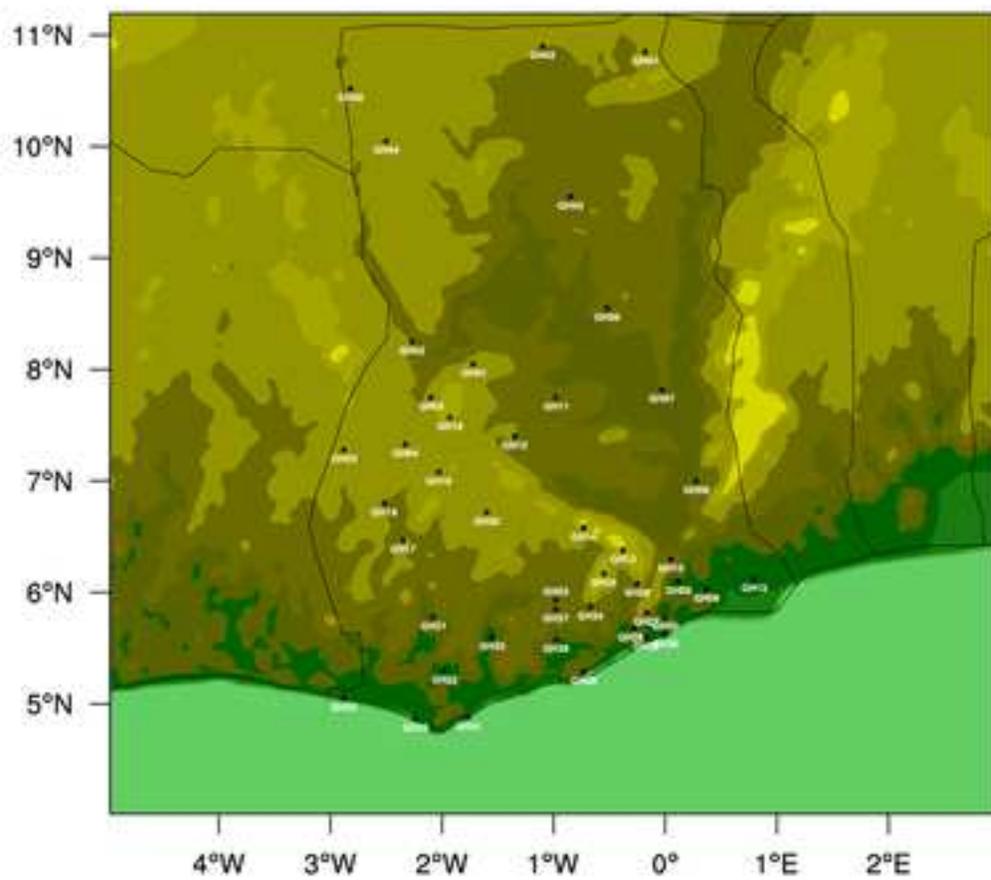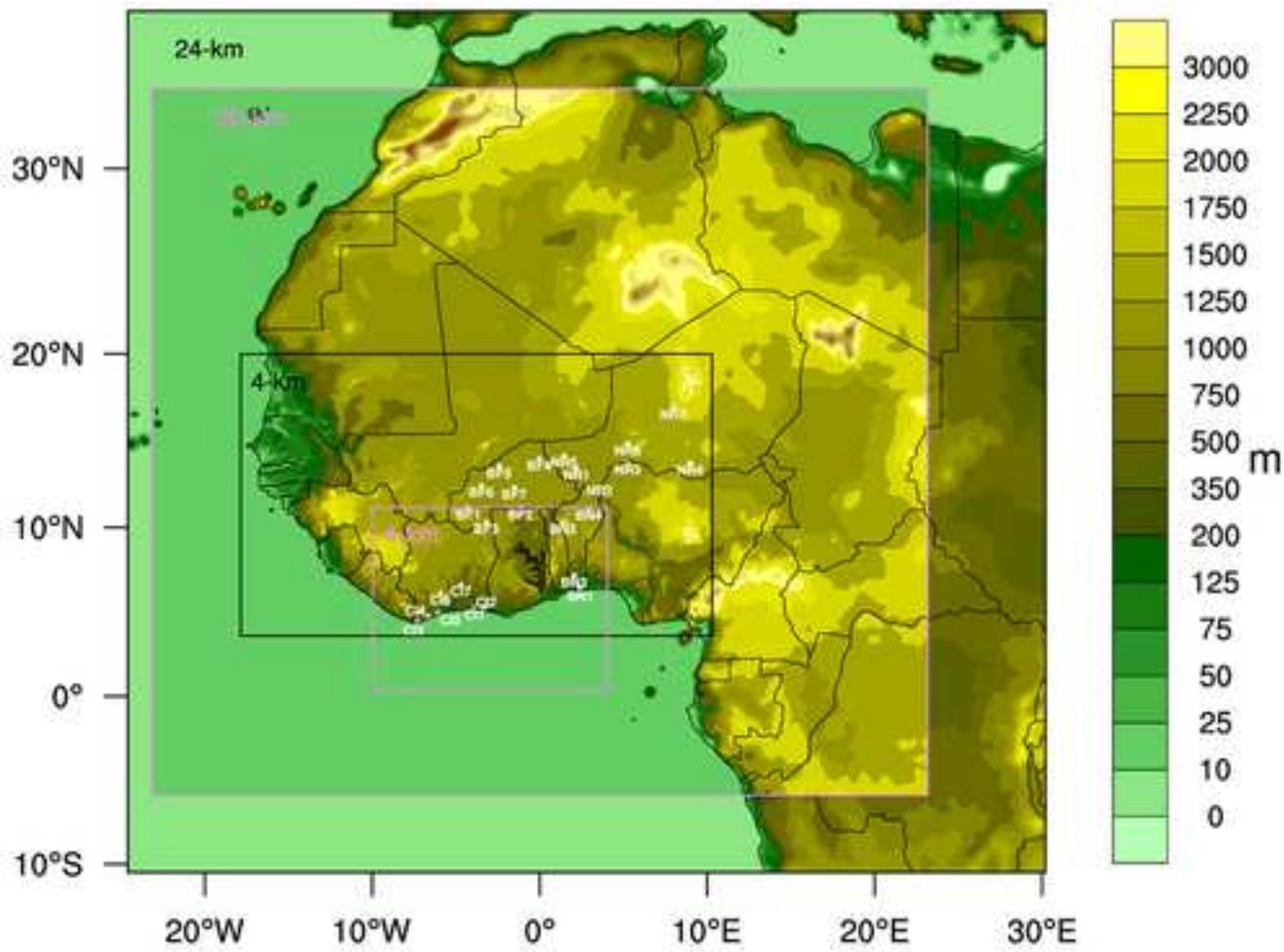993   Mon Weather Rev 136:5095–5115

994 Trenberth KE, Stepaniak DP, Caron JM (2000) The global monsoon as seen through the divergent
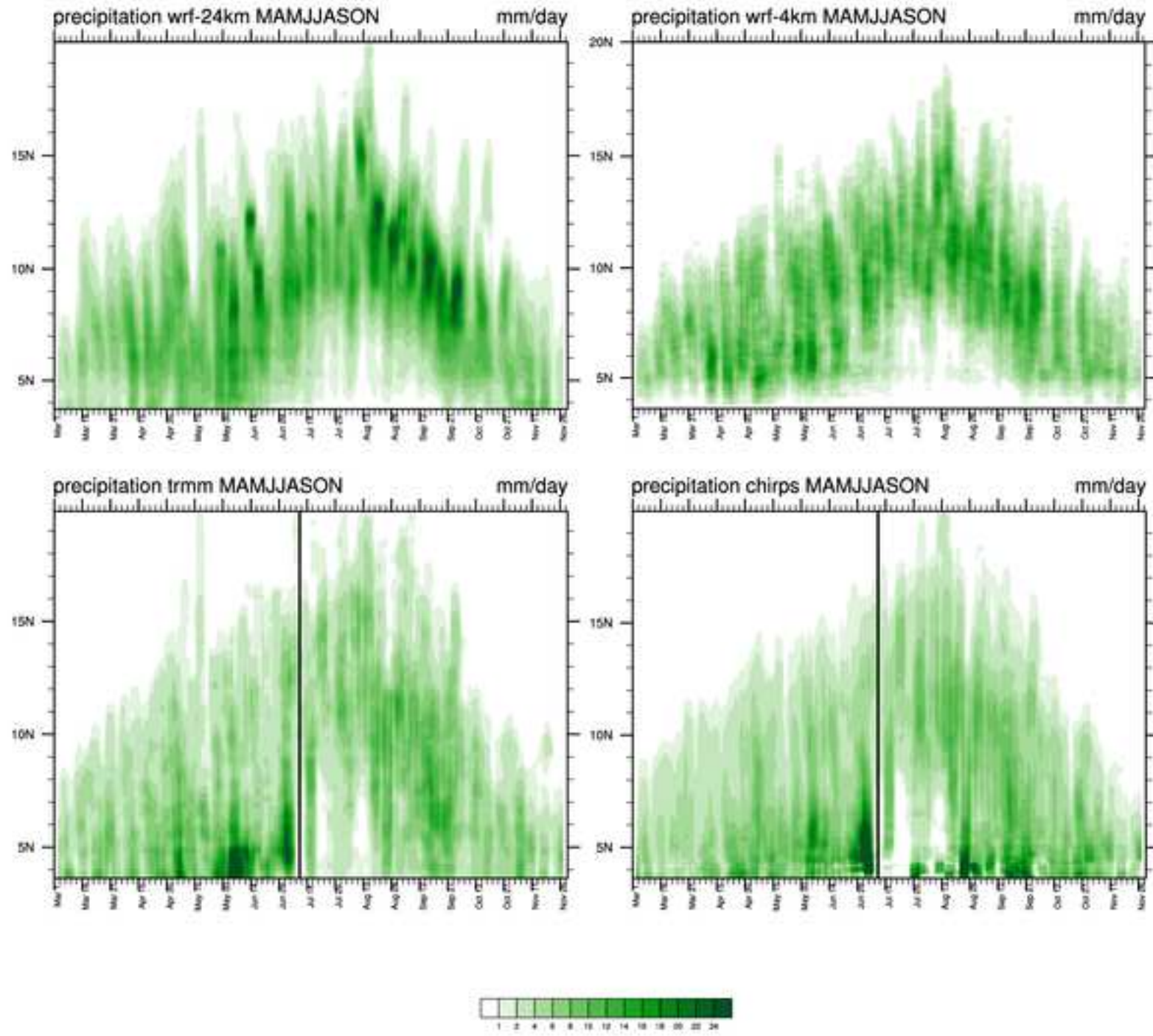995   atmospheric circulation. J Clim 13:3969–3993

996 Vizy EK (2002) Development and application of a mesoscale climate model for the tropics: Influence of
997   sea surface temperature anomalies on the West African monsoon. J Geophys Res 107:. doi:
998   10.1029/2001JD000686

999 Xie B, Fung JC, Chan A, Lau A (2012) Evaluation of nonlocal and local planetary boundary layer
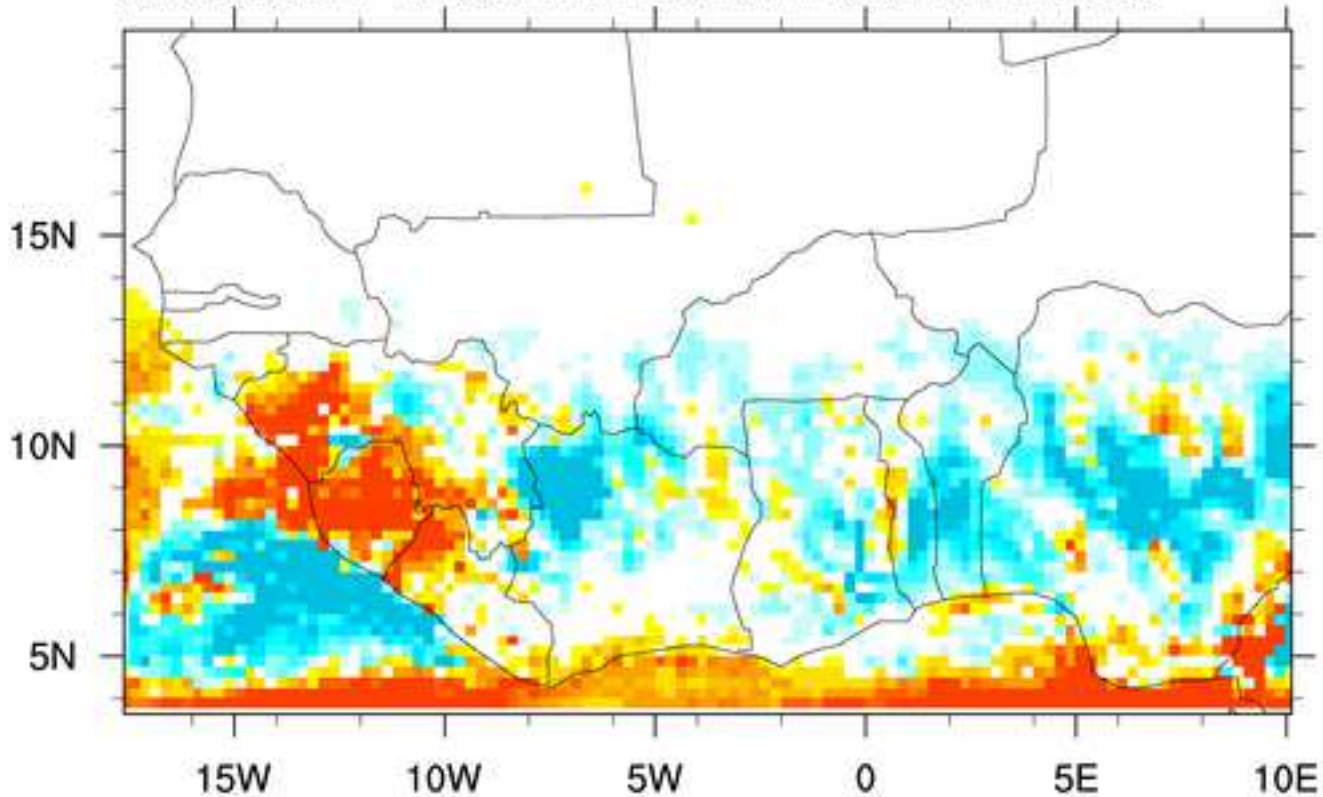1000   schemes in the WRF model. J Geophys Res Atmospheres 1984–2012 117:

1001 Zhang C, Woodworth P, Gu G (2006) The seasonal cycle in the lower troposphere over West Africa from
1002   sounding observations. Q J R Meteorol Soc 132:2559–2582

1003

added value WRF-4km to wrf-24km mean March-November trmm as ref.

added value WRF-4km to wrf-24km mean March-November chirps as ref.

Moisture flux convergence (s^-1)